

Switching Reversibility to Irreversibility in Glycogen Synthase Kinase 3 Inhibitors: Clues for Specific Design of New Compounds

Daniel I. Perez,[†] Valle Palomo,[†] Concepción Pérez,[†] Carmen Gil,[†] Pablo D. Dans,[‡] F. Javier Luque,[§] Santiago Conde,[†] and Ana Martínez^{*,†}

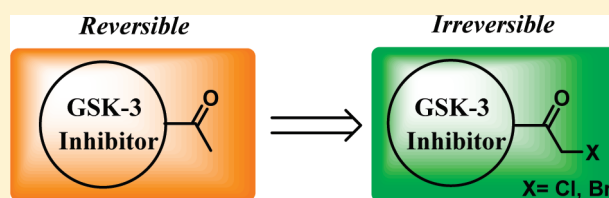
[†]Instituto de Química Medica-CSIC, Juan de la Cierva 3, 28006 Madrid (Spain)

[‡]Biomolecular Simulations Group, Institut Pasteur de Montevideo, Mataojo 2020, 11400 Montevideo (Uruguay)

[§]Departamento de Físicoquímica e Instituto de Biomedicina (IBUB), Facultad de Farmacia, Universidad de Barcelona, Avda. Diagonal 643, 08028 Barcelona (Spain)

S Supporting Information

ABSTRACT: Development of kinase-targeted therapies for central nervous system (CNS) diseases is a great challenge. Glycogen synthase kinase 3 (GSK-3) offers a great potential for severe CNS unmet diseases, being one of the inhibitors on clinical trials for different tauopathies. Following our hypothesis based on the enhanced reactivity of residue Cys199 in the binding site of GSK-3, we examine here the suitability of phenylhalomethylketones as irreversible inhibitors. Our data confirm that the halomethylketone unit is essential for the inhibitory activity. Moreover, addition of the halomethylketone moiety to reversible inhibitors turned them into irreversible inhibitors with IC₅₀ values in the nanomolar range. Overall, the results point out that these compounds might be useful pharmacological tools to explore physiological and pathological processes related to signaling pathways regulated by GSK-3 opening new avenues for the discovery of novel GSK-3 inhibitors.



INTRODUCTION

Protein kinases are important targets for cancer, inflammatory diseases, diabetes, and neurodegenerative disorders, because aberrant protein kinase signaling is implicated in many of these human diseases.¹ To date, ten protein kinase (PK) inhibitors are in clinical use for different cancer treatments.² While some of these agents are active in a subset of patients, most of them develop resistance within the course of one year. To overcome such a problem, irreversible PK inhibitors are gaining importance³ as a new class of therapeutic agents. This knowledge is now being applied to other therapeutic areas such as inflammatory and neurodegenerative pathologies, where PK inhibitors have not reached clinical use yet.

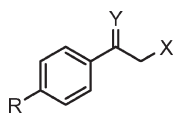
Although several candidate therapeutics for PKs in the central nervous system (CNS) are now in different preclinical and clinical stages,⁴ the development of kinase-targeted therapies for CNS diseases remains a challenge. Specifically inhibition of kinases that phosphorylate tau protein could be beneficial for neurodegenerative diseases.⁵ Among them, glycogen synthase kinase 3 (GSK-3) and cyclin-dependent kinase 5 (CDK-5) play a major hyperphosphorylating role *in vivo*.⁶ GSK-3 inhibitors offer a valuable approach for a future therapy against Alzheimer's disease (AD).^{7–9} Thus, abnormally high GSK-3 activity found in AD patient brains accounts not only for tau hyperphosphorylation, but also for memory impairment, increased β -amyloid production and local plaque-associated microglial-mediated inflammatory responses, which are characteristic hallmarks of the

disease.¹⁰ Recently, the reversion of these pathological features *in vivo* has been shown after oral treatment with a GSK-3 inhibitor in a double transgenic animal model of AD.¹¹

Many drug discovery programs are focused on the development of selective GSK-3 inhibitors. The discovery of non ATP-competitive inhibitors with high GSK-3 specificity is particularly challenging in order to minimize unfavorable off-target effects. In this context, allosteric GSK-3 modulation, as suggested for the basic alkaloid manzamine,^{12,13} or GSK-3 substrate competition,¹⁴ as noted for a small peptide in a study for diabetes, have been valuable strategies to modulate the activity of GSK-3. Other approaches to target GSK-3 avoiding ATP competition have also been envisaged. Specifically, on the basis of previous studies on GSK-3 inhibitors,^{15,16} we have recently hypothesized a new way to selectively target this important kinase based on the existence of a cysteine (Cys199) located in the ATP binding site.¹⁷ Since Cys199 in GSK-3 is replaced by different amino acids in other structurally related kinases, such as CDK-1, CDK-2, or CDK-5, this approach would offer the possibility to design specific drugs via covalent modification of this key residue. Indirect support for this strategy comes from the inhibitory activity determined for thienylhalomethylketones and thiadiazolidindiones (TDZDs),¹⁸ which are the first reported non ATP-competitive GSK-3 inhibitors.¹⁹ Among TDZDs, tideglusib (formerly known as NP-12) is now

Received: December 22, 2010

Published: April 18, 2011

Table 1. GSK-3 Inhibitory Activity of HMKs and Related Compounds

no	X	R	Y	IC ₅₀ (μM)
1 ^a	Cl	H	O	50
2 ^a	Br	H	O	5.0
3 ^a	Cl	Cl	O	2.5
4 ^a	Br	Cl	O	1.0
5 ^a	Br	Br	O	0.5
6 ^a	Br	Me	O	2.5
7 ^a	Br	Ph	O	2.5
8 ^a	Br	OMe	O	1.0
9 ^a	Br	NO ₂	O	2.0
10	I	Br	O	3.0
11	phthalimide	Br	O	100
12	NH ₂	Br	O	100
13	SEt	Br	O	>10
14	SPh	Br	O	>100
15	SBn	Br	O	>10
16	OCOMe	Br	O	>100
17	OH	Br	O	>100
18	Br	Br	NOH	>100
19	Br	Br	NOMe	50
20	Cl	Br	SO	>100

^a See ref²¹

in phase II clinical trials both for AD and for an orphan tauopathy called progressive supranuclear palsy (PSP).

Simultaneously with the writing of this manuscript, some data underlying the importance of cysteine identification on the kinase nucleotide binding site for the design of covalent specific protein kinase inhibitors have been reported.²⁰

Our aim here is to examine the suitability of targeting Cys199, at the entrance of the ATP binding site of GSK-3, as a new drug discovery strategy to develop compounds useful as selective pharmacological tools against this important protein kinase. To this end, we first report the synthesis and biological characterization of phenylhalomethylketones chosen as bioisosters of the irreversible inhibitors previously described in our studies.^{17,21} Moreover, based on X-ray crystallographic and molecular modeling data of GSK-3 complexes, the suitability of our strategy is reinforced by switching compounds with reversible inhibitory properties into irreversible inhibitors. This strategy led us to design, synthesize, and evaluate chemically diverse GSK-3 inhibitors with different kinetics regarding this enzyme. Overall, the results support the implications of Cys199 in the irreversible inhibition of GSK-3 and discover new clues for the synthesis of novel inhibitors for the treatment of human neurodegenerative diseases.

RESULTS AND DISCUSSION

Lead Modification and Structure–Activity Relationship. Screening of our compound library led to the discovery of thienylhalomethylketones as GSK-3 inhibitors.²¹ This behavior

was reinforced by the inhibitory activity found for a small set of commercially available 4-substituted chloro and bromoacetylphenyl derivatives (1–9), as expected from the known bioisosterism between thiophene and benzene rings. Although these compounds showed an interesting range of activities, no clear relationship could be identified between the chemical features of the *para*-substitution and the biological activity (Table 1).

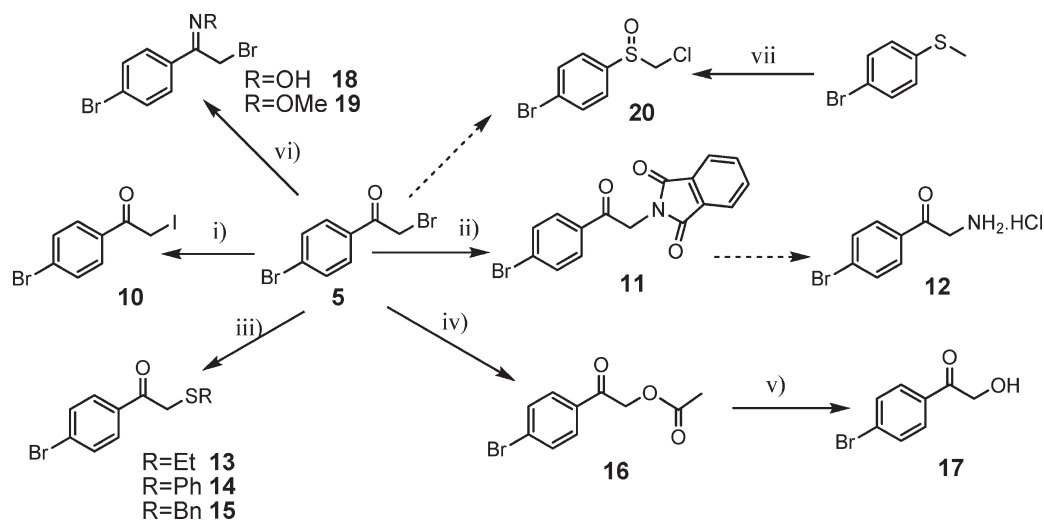
To gain insight into the structure–activity relationships of phenylhalomethylketones as GSK-3 inhibitors, a chemically more diverse set of molecules was evaluated using the 4-bromo-substituted derivative 5 as lead compound due to its high inhibitory activity (IC₅₀ = 0.5 μM). The novel derivatives were designed to explore the influence played by the nature of the halide atom and/or the carbonyl group, which were replaced by different heteroatoms or moieties such as iodine (10), oxygen (16, 17), nitrogen (11, 12), sulfur (13–15), sulfur monoxide (20), oxime (18), and alkyloxime (19) (Scheme 1).

The GSK-3 inhibitory activity was measured following a previously described method that uses [γ -³²P]ATP and the small peptide GS-1 (based on residues of glycogen synthase phosphorylated by GSK-3) as substrate.²² Among the different chemical modifications examined here, only replacement of the bromo acetyl moiety in compound 5 by the iodoacetyl one in 10 retained the inhibitory activity (IC₅₀ = 3.0 μM). All the other compounds did not show significant inhibitory activity (Table 1). Therefore, these findings point out that the halomethylketone (HMK) moiety is a chemical feature necessary for the inhibition of GSK-3.

To further examine the influence of the substituent in the benzene ring, different commercial acetophenones were converted to their bromomethylketo derivatives (21, 23, 25, and 27) by bromine treatment in chloroform at low temperature (Scheme 2). In some cases, the dibromo methyl keto compound (22, 24, 26, and 28) was also isolated. When *p*-aminoacetophenone was used as starting material, bromination not only in the methylketone group but also in the benzene ring was obtained (29). Furthermore, the benzene ring was replaced by the π -deficient 2-pyridine heterocycle, and bromination of 2-acetylpyridine yielded the dibromo derivative 30. In all cases, an IC₅₀ value in the micromolar range was found (Table 2), thus reinforcing the assumption that the bromoacetyl moiety is the key structural feature responsible for the inhibitory activity.

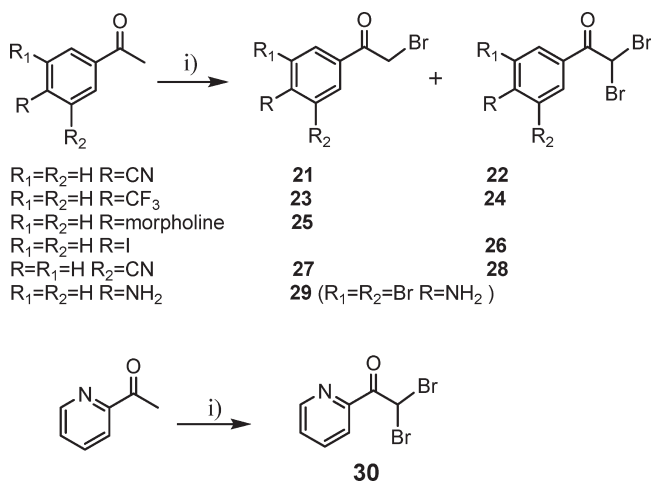
Chemical Reactivity of Phenylhalomethylketones versus Thiol Group. It can be hypothesized that the GSK-3 inhibitory activity of haloacetylphenyl derivatives stems from the reactivity of the HMK moiety with the thiol unit of Cys199, which is located in the ATP binding site. It is therefore necessary to characterize the potential reactivity of haloacetylphenyl compounds in front of thiol groups. To this end, we have analyzed by HPLC–MS the reaction of compound 3 or 4 with 2-mercaptoethanol at room temperature (Table 3). The reaction afforded 11% and 20% of the S-alkylated product for 3 and 4, respectively, in a 1:1 mix ratio after 1 h. When the mixture was stirred for 18 h, the yield of the S-alkylation was 74% and 50%, respectively. When the concentration of mercaptoethanol was increased 10-fold, 78% and 100% of the S-alkylated product was formed after 18 h. On the other hand, upon addition of a tertiary amine, such as triethylamine, at equimolar concentrations of compound 3 or 4 and mercaptoethanol, the S-alkylated product was formed in 65% (3) and 66% (4) after 1 h. The mixture was stirred for 18 h, but a significant increase of the S-alkylated product was not observed. Overall, the results confirm the susceptibility

Scheme 1



(i) KI, acetone, Δ ; (ii) potassium phthalimide, AcN, Δ ; (iii) RSH, K_2CO_3 , EtOH; (iv) $(AcO)_2O$, NaAcO, AcOH, Δ ; (v) CAL-B, $tBuOH$:citrate-phosphate buffer (9:1); (vi) $NH_2OH \cdot HCl$ or $NH_2OMe \cdot HCl$, EtOH, pyr; (vii) SO_2Cl_2 , $AgNO_3$, AcN.

Scheme 2.



(i) Br_2 , $CHCl_3$, 0 °C.

of phenylhalomethylketones to react with thiol groups and the enhanced reactivity upon addition of a suitable base, which might presumably enhance the nucleophilicity of the sulfur atom.

Turning Reversible Inhibitors into Irreversible Inhibition.

To confirm the implication of Cys199 in the inactivation of GSK3 by incubation with phenylhalomethylketones, we checked the possibility of turning reversible inhibitors into irreversible ones upon addition of the HMK unit in a proper position that facilitates the reaction with the thiol group of Cys199. To this end, three structurally distinct compounds were selected taking advantage of the known binding mode to GSK-3 from the X-ray crystallographic structures deposited in the Protein Data Bank: an analogue of ATP (PDB entry 1J1B), and two reversible inhibitors (PDB entries 3F88 and 1R0E). Accordingly, three classes of HMK-containing compounds—derivatives of adenine (**31**, **32**), benzimidazole (**35**, **36**), and maleimide (**37**–**40**)—were considered for chemical modification with Cys199 (Figure 1).

Table 2. GSK-3 Inhibitory Activity of Bromoacetyl Aryl Derivatives

No.	R	R ₁	R ₂	X	Y	IC ₅₀ (μM)
5	Br	H	H	CH	H	0.5
21	CN	H	H	CH	H	1.5
22	CN	H	H	CH	Br	1.5
23	CF ₃	H	H	CH	H	5.0
24	CF ₃	H	H	CH	Br	5.0
25		H	H	CH	H	6.0
26	I	H	H	CH	Br	2.0
27	H	H	CN	CH	H	1.0
28	H	H	CN	CH	Br	1.0
29	NH ₂	Br	Br	CH	Br	0.5
30	H	H	H	N	Br	2.5

The feasibility of this strategy was first explored by means of docking calculations, which were performed using *rDock* (see Experimental Section. Molecular Modeling). The reliability of *rDock* was assessed by docking a set of known GSK-3 inhibitors taking advantage of the X-ray crystallographic structures of their complexes with the enzyme (PDB entries 1J1B, 3F88, 1R0E,

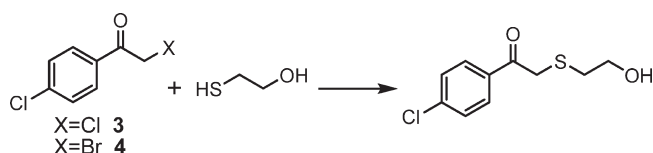
1Q5K, 1UV5, and 2O5K). It is noteworthy that the unrestrained docking protocol was able to predict satisfactorily the X-ray orientation of the compounds in five out of the six cases, as the experimental binding mode was identified as the first or second ranked pose with root-mean-square deviations less than 1.8 Å (see Table S1 in Supporting Information). The X-ray binding mode of the ATP analogue had a higher rank (PDB entry 1J1B), as expected from the larger flexibility of the phosphodiester chain (see Table S1). Inspection of the predicted poses derived for docking calculations for compounds **32**, **36**, and **40** revealed the existence of ligand orientations in the binding site that yielded the HMK moiety suitably positioned for chemical modification by Cys199. This is illustrated for **36** in Figure 2 (see also Figure S1 for compounds **32** and **40**), which shows the second

best pose of the compound, which places the C_α atom of the HMK moiety at around 3.6 Å from the sulfur atom in Cys199).

N-Acylation of adenine was achieved by treatment of acetic anhydride and pyridine in DMSO²³ at room temperature overnight (Scheme 3). The precipitate formed was filtered and washed with cold pyridine and ether to achieve the desired product **31** (51% yield). No bromoacetyl derivative of compound **31** was obtained after treatment of this compound with bromine either at low temperature or reflux. In order to synthesize the haloacetyl derivative **32** of compound **31**, reaction was carried out employing adenine, pyridine, and chloroacetic anhydride in THF.

The synthesis of benzimidazole compounds is described in Scheme 4.²⁴ 1-Bromo-2-nitro-4-acetyl-benzene was treated with

Table 3. Formation of S-Alkylated Products in the Reaction of Compounds **3** and **4** with Mercaptoethanol



reaction conditions	1 h		18 h	
	SM ^a	FP ^b	SM ^a	FP ^b
3:SHEtOH 1:1	88%	11%	24%	74%
3:SHEtOH 1:10	81%	19%	20%	78%
3:SHEtOH:Et ₃ N 1:1:1	33%	65%	34%	65%
4:SHEtOH 1:1	80%	20%	50%	50%
4:SHEtOH 1:10	47%	53%	---	100%
4:SHEtOH:Et ₃ N 1:1:1	33%	66%	25%	75%

^aSM: starting material (compound **3** or **4**). ^bFP: Final product (S-adduct).

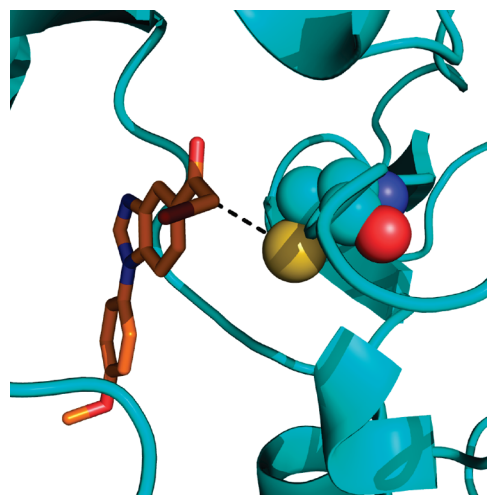


Figure 2. Docked pose for compound **36** with the haloacetyl moiety suitably positioned for chemical modification by Cys199 (shown in spheres; distance from S atom in Cys199 to the C_α atom around or less than 4 Å).

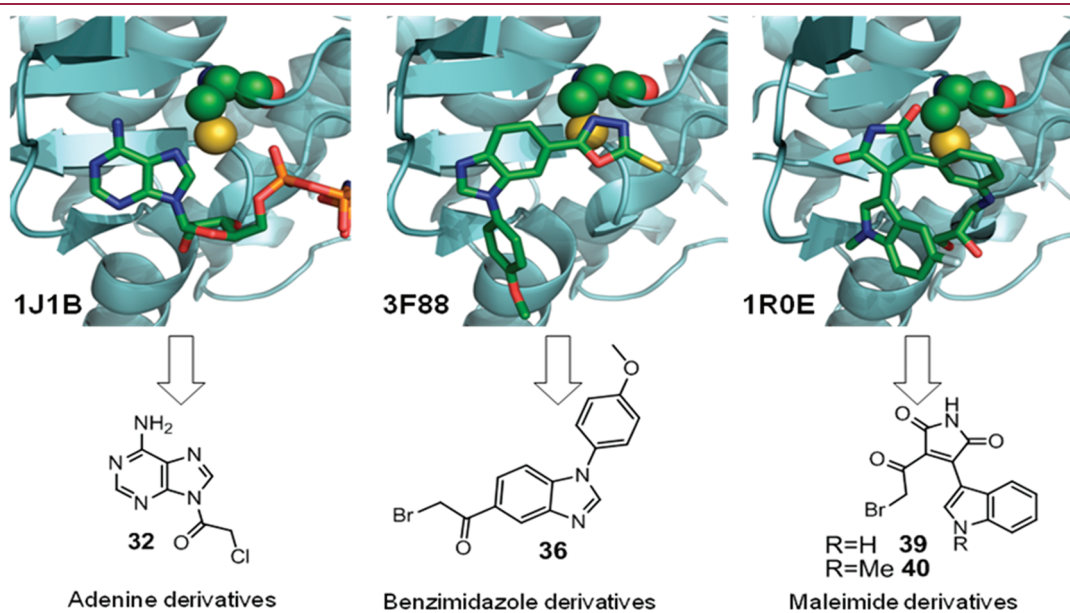
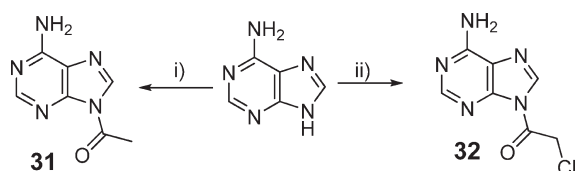


Figure 1. (Top) Representation of the binding mode of an ATP analogue (1J1B), and two reversible inhibitors (3F88 and 1R0E; shown in sticks) in the ATP-binding site of GSK-3. Cys199 is shown in spheres. (Bottom) Structure-based design of novel compounds with potential GSK-3 inhibitory activity.

4-methoxyaniline and sodium acetate in DMF to obtain compound **33** in good yield (73%) after recrystallization. The nitro moiety was reduced under catalytic hydrogenation conditions to yield quantitatively derivative **34**. Final cyclization to synthesize benzimidazole **35** was achieved employing formic acid and HCl 4 N solution. The desired halomethylketone **36** was obtained by reaction of the benzimidazole **35** with bromine in acetic acid under reflux.

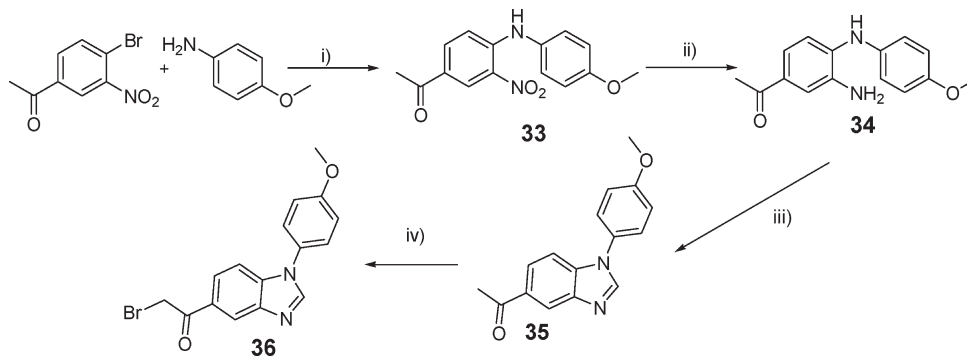
Finally, the direct formation of the maleimide moiety was chosen for synthesis of maleimide derivatives (Scheme 5).²⁵ Because commercial indole products required to synthesize those compounds do not contain a fluorine atom in their structure, we eliminated the fluorine atom from the structure originally proposed. The reaction conditions were carefully optimized to avoid the formation of the major byproduct indoleglyoxylic acid. Thus, methyl 2-indoleglyoxylate or 2-(1-methyl-indol)-glyoxylate was added to a solution of potassium *tert*-butoxide and acetamide in tetrahydrofuran at $-60\text{ }^{\circ}\text{C}$. Under these conditions, compound **37** was obtained with good yield (74%), whereas the methyl indole compound **38** reached 56% yield. These compounds were treated with bromine in acetic acid under reflux to yield HMK compounds **39** and **40**, respectively.

Scheme 3



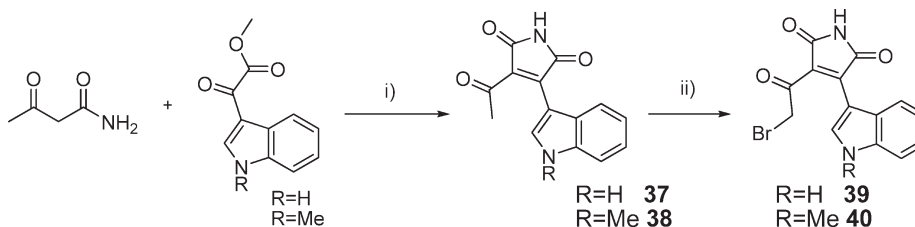
(i) Acetic anhydride, DMSO, rt; (ii) Chloroacetic anhydride, THF, rt.

Scheme 4



(i) Sodium acetate, DMF, $100\text{ }^{\circ}\text{C}$; (ii) H_2 , Pd(C), 20 psi THF, rt; (iii) Formic acid, HCl; (iv) Br_2 , acetic acid, Δ .

Scheme 5



(i) BuOK , THF, $-60\text{ }^{\circ}\text{C}$ to $20\text{ }^{\circ}\text{C}$; (ii) Br_2 , acetic acid, Δ .

All the newly prepared acetyl and halomethylketo heterocycles **31**, **32**, and **35–40** were evaluated as GSK-3 inhibitors using a recently well described luminescent technique²⁶ as a safer nonradioactive assay (see Table 4). The four HMK-containing compounds (**32**, **36**, **39**, and **40**) are more potent than their corresponding acetyl derivatives (**31**, **35**, **37**, and **38**, respectively), showing in one case an IC_{50} value in the nanomolar range.²⁷ More importantly, the inhibitory activity determined at different preincubation times confirmed the switch from reversible to irreversible inhibition (Figure 3). Thus, the inhibition of the acetyl-containing compounds **37** and **38** remained unaltered at different preincubation times, mimicking the behavior of alsterpaullone, a known reversible inhibitor. In contrast, the enzyme inhibition increased with preincubation time for the thiophene irreversible inhibitor **HMK-32**¹⁷ and for the HMK-containing compounds **36**, **39**, and **40**. Overall, these findings are in agreement with our working hypothesis, which provides new clues for the specific design of irreversible GSK-3 inhibitors.

The covalent binding of compound **40** to GSK-3 was confirmed biophysically by MALDI-TOF analyses.²⁸ Compounds **38** and **40** were added in two different experiments to the GSK-3 enzyme under the same conditions as that used for

Table 4. GSK-3 Inhibition Values and Binding Mode of Computer Aided-Designed New Inhibitors

no.	IC_{50} (μM)	binding mode	no.	IC_{50} (μM)	binding mode
31	>50	---	35	>10	---
32	13.4	irreversible	36	0.58 ± 0.07	irreversible
37	4.47 ± 0.35	reversible	38	0.89 ± 0.19	reversible
39	0.047 ± 0.007	irreversible	40	0.005 ± 0.001	irreversible

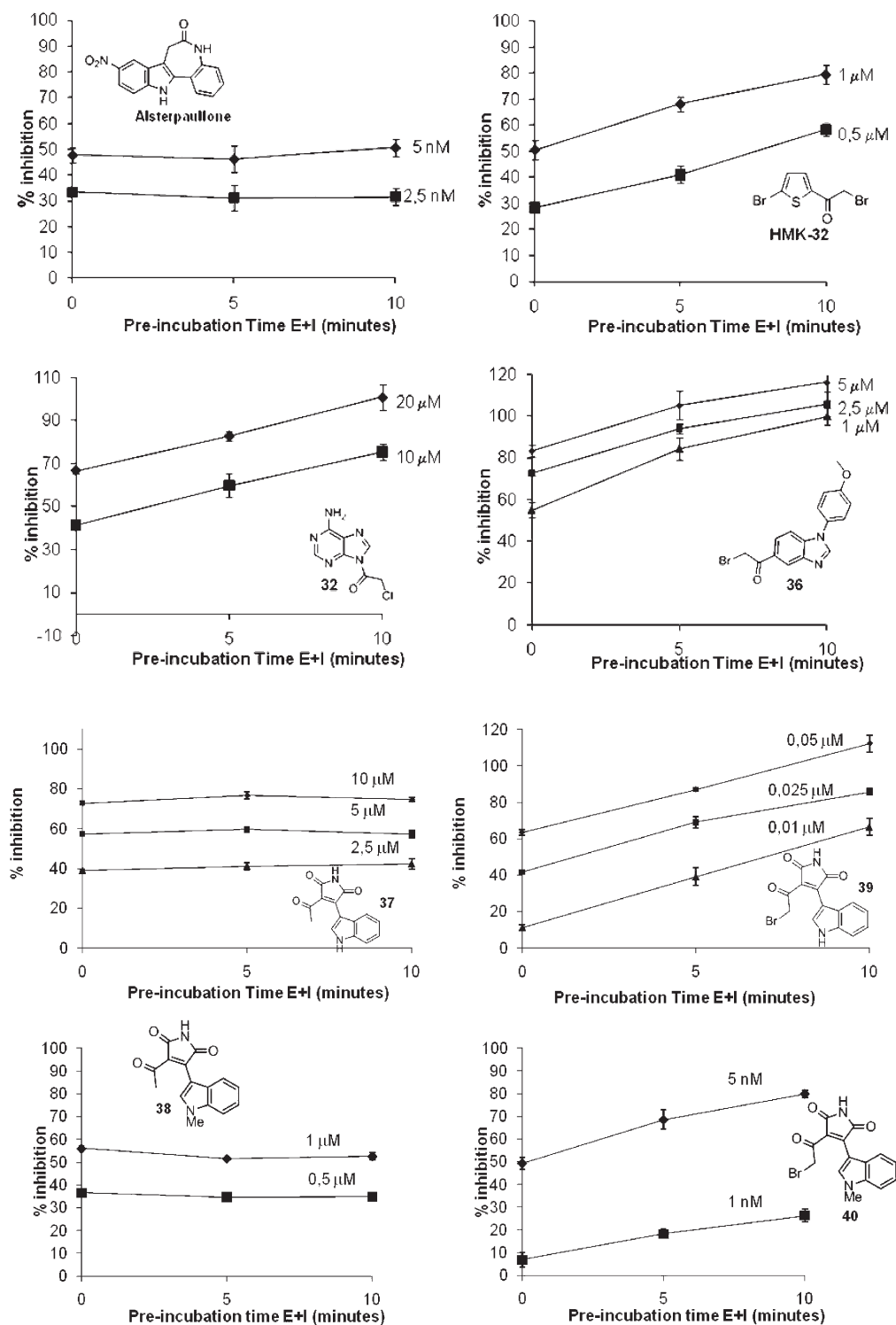


Figure 3. Time-dependent GSK-3 inhibition of controls (alsterpaullone and HMK-32) and the newly synthesized protein kinase inhibitors.

IC₅₀ measurements. Mass analysis revealed that, when the reversible inhibitor **38** was used, only the mass corresponding to GSK-3 (48794 Da) was detected, whereas the use of an irreversible inhibitor (compound **40**) showed a mass peak of 49036 Da confirming its covalent irreversible binding to the enzyme (Figure 4).

Cellular Effects of Phenylhalomethylketones on GSK-3 Inhibition. All the preceding results suggest that phenylhalomethylketones may be versatile pharmacological tools to explore

GSK-3-mediated cellular processes in physiological or pathological conditions. As GSK-3 is involved in tau phosphorylation in transfected cells and *in vivo*,²⁹ we further explored their ability to interfere with the GSK-3 mediated tau phosphorylation in cells using primary granule cerebellar neurons (GCNs), which also allow us to evaluate the cell permeability of the new inhibitors.

The effect on tau phosphorylation was determined by Western blotting, and detection was carried out using specific

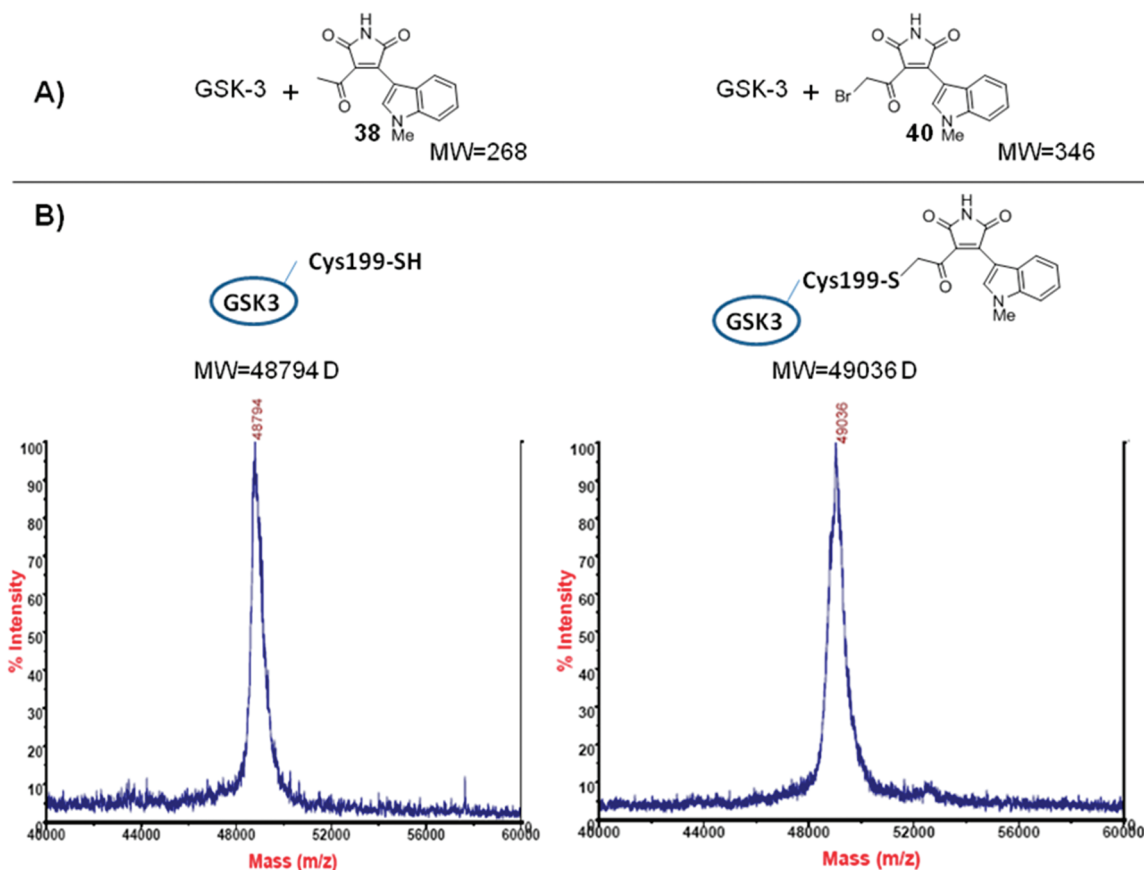


Figure 4. MalDI-TOF spectra. (A) Reversible inhibitor **38** (MW = 268) with GSK-3 (MW = 48 794) showed a 48 794 mass peak. (B) Irreversible inhibitor **40** (MW = 346) with GSK-3 showed a 49 036 mass peak corresponding to the covalent bond S–C formed between the GSK-3 enzyme and the inhibitor **40**.

antibodies: Tau-1 for tau immunoreactivity, and PHF-1 as tau phosphospecific Ser396 reagent. This last epitope is specifically phosphorylated by GSK-3 on tau protein.³⁰ Lithium chloride, the first reported GSK-3 inhibitor, was used as standard reference and was added as positive control to the medium at 20 mM. The bands were quantified by densitometric analysis. Following this procedure, data showed that the addition of phenylhalomethylketone **6** or **8** reduced (PHF-1) or increased (Tau-1) the tau-immunoreactivity, thus mimicking the effect observed when lithium chloride was used as a GSK-3 inhibitor ($IC_{50} = 1.5$ mM) (Figure 5).

Kinase and Neurotransmitter Binding Profiles of Phenylhalomethyl Ketones. To examine the PK selectivity of phenylhalomethylketones for GSK-3, compounds **3**, **5**, and **6** were tested as inhibitors of serine/threonine cAMP-dependent protein kinase (PKA). All of them remained inactive at the highest concentration (100 μ M) used. Furthermore, the same set of compounds was evaluated against a panel of eight different serine/threonine and tyrosine kinases (CaM-K II, MAP-K, EGFR-K, IR-K, MeK1-K, Abl-K, PKp56, and Src), which are involved in very different signaling pathways not only in neurodegeneration (Cam-KII and MAP-K), but also in other physiological processes and diseases, such as insulin signal pathway (IR-K) or cancer (Abl-K, EGFR-K, MeK1-K, and Src). The inhibitory assays (performed using a 10 μ M concentration for the different compounds) showed that, in general, HMKs did not exhibit a significant inhibitory effect on the whole set of kinases (Table 5).

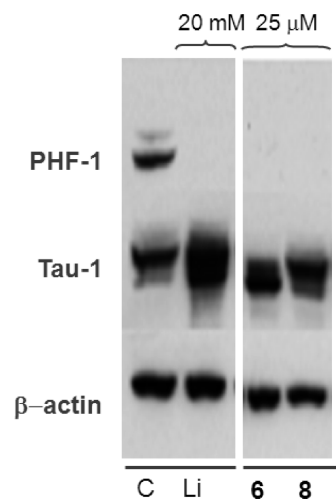


Figure 5. Representative Western blot of soluble extracts from Granule cerebellar neurons (GCNs), obtained after 16 h in the presence of lithium chloride (Li) or different phenylhalomethylketones (**6** and **8**). C represents cell extracts from control GCNs. Identical samples were incubated with antitau-1, anti PHF-1, or anti- β -actin, which was used as a loading control. In each experiment, PHF-1 was normalized with respect to the amount of actin present in each cell extract.

Only the proto-oncogenic Src, which is elevated in some human tumors, is smoothly inhibited by the three selected compounds.

Table 5. Inhibitory Activity (% Inhibition)^a Shown by Selected Phenylhalomethylketones for Several Kinases

compound (10 μ M)	Abl-K	Cam-KII	EGFR-K	IR-K	MAP-K	MEK-1 K	PK p56	Src-K
3	–	16	–	–	–	–	–	19
5	–	–	18	–	–	–	29	38
6	–	15	10	–	–	–	38	69

^a The symbol – indicates an inhibitory activity of less than 10%.

Table 6. Inhibitory Activity (% Inhibition)^a Exhibited by Selected Phenylhalomethylketones for Neurotransmitter Receptors

compound (10 μ M)	α_2	hD2	hD3	AMPA	NMDA	hM	N (α BGT insensitive)	N (α BGT sensitive)	5-HT
3	–	–	–	–	15	–	–	–	–
5	–	–	–	–	–	–	16	–	–
6	10	–	–	–	–	13	–	–	–

^a The symbol – indicates inhibitory activity of less than 10%.

Furthermore, it is also important for pathway analysis *in vivo* and in cellular systems to evaluate the potential off-target effects of these new pharmacological tools. This is of particular relevance in phenylhalomethylketones due to the presence of a potential reactive group in their chemical structure, which might react with different neurotransmitter receptors, thus masking a neat GSK-3 response. In order to determine the potential off-target effects of these compounds, we evaluated the *in vitro* binding to different neurotransmitter receptors: α -adrenergic (α_2), dopaminergic (hD2 and hD3), glutamatergic (AMPA and NMDA), muscarinic (hM), nicotinic (bungarotoxin sensitive and insensitive), and serotonergic (5-HT) receptors. Results showed that compounds 3, 5, and 6 (at 10 μ M concentration) did not bind to any of these neurotransmitter receptors (Table 6).

CONCLUSIONS

GSK-3 is a therapeutically valuable kinase that is very promising for severe unmet diseases such as AD. To the best of our knowledge, only a small molecule acting as GSK-3 inhibitor, the TDZD compound called Tideglusib, has reached phase IIb clinical trials for the treatment of AD. Additionally, lithium is used in the clinic as the first option for treatment of bipolar disorders, and it is known to inhibit GSK-3 among other mechanisms of action.

The irreversible inhibition of GSK-3 reported for thienylhalomethylketones was suggested to involve covalent modification of Cys199,¹⁷ which is located in the ATP-binding site. Modification of Cys199 might then be a new strategy for the design of specific GSK-3 inhibitors. At this point, the series of phenylhalomethylketone derivatives examined confirms unequivocally the key role of the HMK moiety on GSK-3 inhibition. Furthermore, the implication of Cys199 is supported by the structure-based design of novel compounds characterized by reversible inhibition, which turn out to be irreversible inhibitors upon addition of an HMK unit to their chemical structure.

Overall, chemical modification of Cys199 represents a new mechanism of action that opens new avenues for the development of potent, selective GSK-3 inhibitors. In this context, it is worth highlighting that phenylhalomethylketones (i) act as cell-permeable inhibitors, (ii) decrease tau phosphorylation in cell cultures, (iii) are rather selective against a panel of protein kinases, and (iv) do not bind to different neurotransmitter receptors. Thus, they may be considered useful pharmacological tools to explore physiological and pathological cellular signaling pathways in which GSK-3 is involved.

These findings are especially relevant, as an emerging aspect in the effectiveness of protein kinases inhibitors *in vivo* is the ability to compete with cellular concentrations of ATP (typically about 1–10 mM). For epidermal growth factor receptor kinase (EGFR-K), such problems have been overcome with compound HKI-272, which binds covalently to a cysteine residue.³¹ A similar strategy has been recently reported for the irreversible inhibition of HCV NS3/4A viral protease by targeting a noncatalytic cysteine residue.³² In this context, the strategy explored here, which relies on the key role of Cys 199 in GSK-3 inhibition, might then represent a promising strategy for the development of novel GSK-3 inhibitors for the treatment of severe human diseases.

EXPERIMENTAL SECTION

Chemistry. *General.* Substrates were either purchased from commercial sources or used without further purification. Melting points were determined with a Reichert-Jung Thermovar apparatus and a Mettler Toledo MP70 apparatus and are uncorrected. Flash column chromatography was carried out at medium pressure using silica gel (E. Merck, grade 60, particle size 0.040–0.063 mm, 230–240 mesh ASTM) with the indicated solvent as eluent. Compounds were detected with UV light (254 nm). ¹H NMR spectra were obtained on a Gemini-200 spectrometer working at 200 MHz and on a Bruker AVANCE-300 spectrometer working at 300 MHz. Typical spectral parameters: spectral width 10 ppm, pulse width 9 μ s (57°), data size 32 K. ¹³C NMR experiments were carried out on the Varian Gemini-200 spectrometer operating at 50 MHz and on the Bruker AVANCE-300 spectrometer operating at 75 MHz. The acquisition parameters: spectral width 16 kHz, acquisition time 0.99 s, pulse width 9 μ s (57°), data size 32 K. Chemical shifts are reported in values (ppm) relative to internal Me₄Si and J values are reported in Hertz. Elemental analyses were performed by the analytical department at CENQUIOR (CSIC), and the results obtained were within \pm 0.4% of the theoretical values. The combustion analyses are provided in the Supporting Information. Mass spectra were obtained by electronic impact in a Hewlett-Packard 5973 spectrophotometer. All compounds are >95% pure by HPLC analyses. HPLC analyses for compounds 10–30 were performed on a Waters 6000 instrument, with UV detector (214–254 nm), using different columns; μ Bondapak C18, 10 μ m, 125 Å, (300 \times 3.9 mm) and Symmetry C18, 5 μ m, 100 Å, (150 \times 3.9 mm). Acetonitrile/H₂O [(0.05% H₃PO₄ + 0.04% Et₃N)] 50/50 was used as mobile phase. For the chemical reactivity of HMKs versus thiol groups and HPLC analyses for compounds 31–40, experiments were performed on Alliance Waters 2690 equipment with a UV detector photodiode array Waters 2996 with MS detector MicromassZQ

(Waters) positive electrospray, using the Sunfire column C18, 3.5 μm (50×4.6 mm) and acetonitrile (0.08% formic acid) and MilliQ water (0.1% formic acid) as mobile phase in a 10 min run from 10% to 100% acetonitrile gradient at a flow rate of 0.25 mL/min.

MALDI-MS measurements were performed on a Voyager DE-PRO mass spectrometer (Applied Biosystems, Foster City, CA) equipped with a pulsed nitrogen laser ($\lambda = 337$ nm, 3 ns pulse width, and 3 Hz frequency) and a delayed extraction ion source. Ions generated by the laser desorption were introduced into a time-of-flight analyzer (1.3 m flight path) with an acceleration voltage of 25 kV, a 88% grid voltage, a 0.3% ion guide wire voltage, and a delay time of 500 ns in the linear positive ion mode.

Mass spectra were obtained over the m/z range 30 000–125 000 u . External mass calibration was applied using the monoisotopic $[M+H]^+$ value of Enolase. Sinapinic acid (>99%; Fluka, Buchs, Switzerland) at 10 mg mL⁻¹ in 0.3% trifluoroacetic acid/acetonitrile, 70:30 (v/v) was used as matrix. Samples were mixed with the matrix at a ratio of approximately 1:1, and 1 μL of this solution was spotted onto a flat stainless steel sample plate and dried in air.

1-(4-Bromophenyl)-2-iodoethanone (10).³³ A mixture of 2-bromo-1-(4-bromophenyl)ethanone (**5**) (2.0 g, 7.20 mmol) and potassium iodide (8.40 g, 50 mmol) in acetone (50 mL) was stirred and refluxed for 3 h. The solvent was evaporated, and CH_2Cl_2 (100 mL) and H_2O (100 mL) were added to the reaction mixture. The organic layer was dried over MgSO_4 and the solvent was evaporated. Compound **10** was purified by silica gel chromatography (hexane:ethyl acetate 6:1), 1.91 g (82%), colorless solid, mp 95–96 °C. ¹H NMR (200 MHz, CDCl_3): δ 7.83 (d, $J = 8.3$ Hz, 2H), 7.60 (d, $J = 8.3$ Hz, 2H), 4.30 (s, 2H). ¹³C NMR (75 MHz, CDCl_3): δ 190.7, 131.6, 129.5, 127.8, 123.7, 24.3. m/z (EI): 326, 324, (M^+ , 12, 13%), 185, 183 (M- CH_2I , 97, 100%). HPLC: Column Symmetry C18, 5 μm , 100 \AA , (150 \times 3.9 mm), Purity 99%, r.t. = 14.15 min, acetonitrile/ H_2O (0.05% H_3PO_4 + 0.04% Et_3N) 50/50.

2-(2-(4-Bromophenyl)-2-oxoethyl)isoindoline-1,3-dione (11).³⁴ A mixture of 2-bromo-1-(4-bromophenyl)ethanone (**5**) (0.3 g, 1.08 mmol) and potassium phthalimide (0.21 g, 1.13 mmol) in acetonitrile (50 mL) was stirred and refluxed for 2 h. The solvent was evaporated, and CH_2Cl_2 (100 mL) and H_2O (100 mL) were added to the mixture. The organic layer was washed with a 0.2 N sodium hydroxide solution (50 mL) and water (50 mL). Then the organic layer was dried over MgSO_4 and the solvent was evaporated. Compound **11** was purified by silica gel chromatography (hexane:ethyl acetate 3:1), 0.28 g (76%), colorless solid, mp 223–225 °C. ¹H NMR (200 MHz, CDCl_3): δ 7.91 (m, 2H), 7.87 (d, $J = 8.4$ Hz, 2H), 7.76 (m, 2H), 7.67 (d, $J = 8.4$ Hz, 2H), 5.01 (s, 2H). ¹³C NMR (75 MHz, CDCl_3): δ 190.1, 167.8, 134.2, 132.2, 129.6, 123.5, 133.1, 132.7, 132.1, 129.4, 44.0. m/z (EI): 345, 343 (M^+ , 21, 21%), 185, 183 (M- CH_2 phthalimide, 98, 100%). HPLC: Column Symmetry C18, 5 μm , 100 \AA , (150 \times 3.9 mm), Purity 99%, r.t. = 3.66 min, acetonitrile/ H_2O (0.05% H_3PO_4 + 0.04% Et_3N) 50/50.

2-Amino-4'-bromoacetophenone hydrochloride (12). Commercially available from Sigma Aldrich.

General Procedure for the Synthesis of Sulfur Derivatives (Compounds 13–15). A mixture of 2-bromo-1-(4-bromophenyl)ethanone (**5**), potassium carbonate, and the corresponding thiol (ethanethiol, thiophenol, and benzylthiol) in ethanol (50 mL) was stirred and refluxed for 2 h. The mixture was filtered, and CH_2Cl_2 (75 mL) and water (75 mL) were added to the solution. The organic layer was washed with water (2 \times 75 mL). Then the organic layer was dried over MgSO_4 and the solvent was evaporated. The compounds were purified by silica gel chromatography.

1-(4-Bromophenyl)-2-(ethylthio)ethanone (13).³⁵ 2-Bromo-1-(4-bromophenyl) ethanone (**5**) (0.5 g, 1.80 mmol), potassium carbonate (0.25 g, 1.80 mmol), ethanethiol (0.11 g, 1.80 mmol). Purified by silica gel chromatography (hexane:ethyl acetate 4:1), 0.20 g (45%), colorless solid, mp 64–65 °C. ¹H NMR (200 MHz, CDCl_3): δ 7.74 (d, $J = 8.7$ Hz,

2H), 7.50 (d, $J = 8.7$ Hz, 2H), 3.65 (s, 2H), 2.46 (q, $J = 14.6$, 7.3 Hz, 3H), 1.16 (t, $J = 7.3$ Hz, 2H). ¹³C NMR (75 MHz, CDCl_3): δ 194.3, 134.7, 132.8, 131.2, 129.4, 37.5, 27.2, 14.9. m/z (EI): 260, 258 (M^+ , 10, 9%), 185, 183 (M-S $\text{CH}_2\text{CH}_2\text{CH}_3$, 100, 99%). HPLC: Column Symmetry C18, 5 μm , 100 \AA , (150 \times 3.9 mm), Purity 99%, r.t. = 5.85 min, acetonitrile/ H_2O (0.05% H_3PO_4 + 0.04% Et_3N) 50/50.

1-(4-Bromophenyl)-2-(phenylthio)ethanone (14).³⁶ 2-Bromo-1-(4-bromophenyl) ethanone (**5**) (0.5 g, 1.80 mmol), potassium carbonate (0.25 g, 1.80 mmol), benzenethiol (0.20 g, 1.80 mmol). Purified by silica gel chromatography (hexane:ethyl acetate 4:1), 0.29 g (53%), colorless solid, mp 60–61 °C. ¹H NMR (200 MHz, CDCl_3): δ 7.68 (d, $J = 8.7$ Hz, 2H), 7.49 (d, $J = 8.7$ Hz, 2H), 7.24–7.20 (m, 5H), 4.10 (s, 2H). ¹³C NMR (75 MHz, CDCl_3): δ 192.8, 134.0, 133.7, 130.4, 130.1, 129.9, 128.8, 128.4, 127.0, 40.7. m/z (EI): 308, 306 (M^+ , 55, 52%), 185, 183 (M-S CH_2Ph , 100, 98%). HPLC: Column Symmetry C18, 5 μm , 100 \AA , (150 \times 3.9 mm), Purity 99%, r.t. = 8.15 min, acetonitrile/ H_2O (0.05% H_3PO_4 + 0.04% Et_3N) 50/50.

2-(Benzylthio)-1-(4-bromophenyl)ethanone (15).³⁷ 2-Bromo-1-(4-bromophenyl) ethanone (**5**) (0.5 g, 1.80 mmol), potassium carbonate (0.25 g, 1.80 mmol), benzylthiol (0.22 g, 1.80 mmol). Purified by silica gel chromatography (hexane:ethyl acetate 4:1), 0.32 g (55%), colorless solid, mp 158–159 °C. ¹H NMR (200 MHz, CDCl_3): δ 7.68 (d, $J = 8.7$ Hz, 2H), 7.49 (d, $J = 8.7$ Hz, 2H), 7.24–7.20 (m, 5H), 3.63 (s, 2H), 3.52 (s, 2H). ¹³C NMR (75 MHz, CDCl_3): δ 192.3, 136.1, 133.0, 130.9, 129.2, 128.3, 127.6, 126.4, 126.3, 35.1, 34.7. m/z (EI): 322, 320 (M^+ , 17, 17%), 200, 198 (M-S CH_2Ph , 85, 83%). HPLC: Column Symmetry C18, 5 μm , 100 \AA , (150 \times 3.9 mm), Purity 99%, r.t. = 9.76 min, acetonitrile/ H_2O (0.05% H_3PO_4 + 0.04% Et_3N) 50/50.

2-(4-Bromophenyl)-2-oxoethyl acetate (16).³⁸ To a solution of 2-bromo-1-(4-bromophenyl)ethanone (**5**) (0.5 g, 1.80 mmol) in acetic acid (50 mL) was added sodium acetate (0.44 g, 5.40 mmol) and acetic anhydride (0.55 g, 5.40 mmol). The mixture was stirred and refluxed for 5 h. CH_2Cl_2 (100 mL) and H_2O (100 mL) were added to the reaction mixture. The organic layer was washed with H_2O (2 \times 100 mL), a saturated solution of NaHCO_3 (100 mL), and a saturated solution of NaCl (100 mL). The organic layer was dried over MgSO_4 and the solvent was evaporated. Compound **16** was purified by silica gel chromatography (hexane:ethyl acetate 7:1), 0.41 g (87%), colorless solid, mp 84–85 °C. ¹H NMR (200 MHz, CDCl_3): δ 7.67 (d, $J = 8.6$ Hz, 2H), 7.35 (d, $J = 8.6$ Hz, 2H), 5.18 (s, 2H), 2.12 (s, 3H). ¹³C NMR (50 MHz, CDCl_3): δ 190.3, 169.3, 131.8, 131.2, 128.2, 128.1, 64.8, 19.5. m/z (EI): 260, 258 (M^+ , 15, 15%), 183, 181, 179 (M-C $\text{H}_3\text{H}_5\text{O}_2$, 25, 89, 100%). HPLC: Column Symmetry C18, 5 μm , 100 \AA , (150 \times 3.9 mm), Purity 100%, r.t. = 6.41 min, acetonitrile/ H_2O (0.05% H_3PO_4 + 0.04% Et_3N) 50/50.

1-(4-Bromophenyl)-2-hydroxyethanone (17).³⁹ Enzymatic deacylation of **16**, was done employing different lipases (PPL (*Pancreatic Porcine Lipase*), PSL (*Pseudomonas cepacia Lipase*), MML (*Mucor miehi Lipase*), and CAL-B (*Candida Antartica Lipase-B*) under the same reaction conditions (citrate-phosphate 9:1 buffer pH 7, *tert*-butanol, 45 °C, 24 h). No product was obtained using MML, while partial hydrolysis was done when lipases PPL and PSL were employed. However, the use of CAL-B gave exclusively compound **17** with an 85% yield. Accordingly, a mixture of 2-(4-bromophenyl)-2-oxoethyl acetate (**16**) (20 mM) and CAL-B (20 mM) in *tert*-butanol:citrate phosphate buffer (pH = 7) 9:1 (85 mL) was orbitally stirred and refluxed for 24 h. The reaction was filtered and ethyl acetate (75 mL) and H_2O (50 mL) were added to the solution. The organic layer was dried over MgSO_4 and the solvent was evaporated. Compound **17** was purified by silica gel chromatography (hexane:ethyl acetate 1:1), 0.36 g (85%), colorless solid, mp 103–104 °C. ¹H NMR (200 MHz, CDCl_3): δ 7.80 (d, $J = 8.6$ Hz, 2H), 7.65 (d, $J = 8.6$ Hz, 2H), 4.85 (s, 2H). ¹³C NMR (75 MHz, CDCl_3): δ 197.8, 132.9, 132.4, 130.1, 129.5, 65.7. m/z (EI): 216, 214 (M^+ , 11, 11%), 185, 183, (M-C H_3O , 100, 100%). HPLC: Column Symmetry

C18, 5 μm , 100 \AA , (150 \times 3.9 mm), Purity 99%, r.t. = 3.81 min, acetonitrile/H₂O (0.05% H₃PO₄ + 0.04% Et₃N) 50/50.

General Procedure for Oxime (18) and Methyl Oxime Synthesis (19). To a mixture of hydroxylamine hydrochloride or methylhydroxylamine hydrochloride and pyridine in ethanol (50 mL) was added 2-bromo-1-(4-bromophenyl)ethanone (5). The mixture was stirred and refluxed for 4 h. The solvent was evaporated and cold water (25 mL) was added to the mixture. The mixture is left at 0 °C for 12 h and the precipitate formed was filtered. The compounds were purified by silica gel chromatography.

(E,Z)-2-Bromo-1-(4-bromophenyl)ethanone Oxime (18).⁴⁰ Hydroxylamine hydrochloride (0.26 g, 3.81 mmol), pyridine (0.31 g, 3.81 mmol), and 2-bromo-1-(4-bromophenyl)ethanone (5) (1.0 g, 3.59 mmol). Purified silica gel column chromatography (hexane:ethyl acetate 6:1), 0.82 g (78%), colorless solid, mp 115–116 °C. ¹H NMR (200 MHz, CDCl₃): δ 11.8, 11.7 (s, 1H), 7.52–7.41 (m, 4H), 4.48, 4.35 (s, 2H). ¹³C NMR (75 MHz, CDCl₃): δ 154.0, 153.9, 132.7, 132.3, 128.2, 124.7, 32.1, 27.2. *m/z* (EI): 295, 293, 291 (M⁺, 36, 72, 38%), 102 (M-CH₃Br₂O, 100%). HPLC: Column Symmetry C18, 5 μm , 100 \AA , (150 \times 3.9 mm), Purity 99%, r.t. = 8.15 min, acetonitrile/H₂O (0.05% H₃PO₄ + 0.04% Et₃N) 50/50.

(E,Z)-2-Bromo-1-(4-bromophenyl)ethanone *O*-Methyl Oxime (19).⁴¹ Methyl hydroxylamine hydrochloride (0.30 g, 3.59 mmol), pyridine (0.28 g, 3.59 mmol), and 2-bromo-1-(4-bromophenyl)ethanone (5) (1.0 g, 3.59 mmol). Purified by silica gel chromatography (hexane:ethyl acetate 6:1), 0.56 g (82%), colorless solid, mp 48–49 °C. ¹H NMR (200 MHz, CDCl₃): δ 7.65–7.51 (m, 4H), 4.52, 4.35 (s, 2H), 4.15, 4.05 (s, 3H). ¹³C NMR (75 MHz, CDCl₃): δ 151.2, 132.4, 131.9, 127.7, 124.1, 63.0, 62.9, 32.2, 32.1. *m/z* (EI): 309, 307, 305 (M⁺, 13, 26, 13%), 102 (M-C₂H₅Br₂O, 100%). HPLC: Column Symmetry C18, 5 μm , 100 \AA , (150 \times 3.9 mm), Purity 99%, r.t. = 8.10 min, acetonitrile/H₂O (0.05% H₃PO₄ + 0.04% Et₃N) 50/50.

1-Bromo-4-(chloromethylsulfanyl)benzene (20).⁴² A solution of sulfuryl chloride (0.33 g, 2.46 mmol) in acetonitrile (5 mL) was added dropwise to a mixture of bromothioanisole (0.50 g, 2.46 mmol) and silver nitrate (0.42 g, 2.46 mmol) in acetonitrile (10 mL) at 0 °C. The mixture was then stirred 1 h at room temperature. CH₂Cl₂ (10 mL) and H₂O (10 mL) were added to the reaction mixture. The organic layer was washed with H₂O (2 \times 100 mL), dried over MgSO₄, and the solvent was evaporated. Compound 20 was purified by silica gel chromatography (hexane:ethyl acetate 1:1), 0.44 g (71%), colorless solid, mp 91–92 °C. ¹H NMR (200 MHz, CDCl₃): δ 7.71 (d, *J* = 8.7 Hz, 2H), 7.58 (d, *J* = 8.7 Hz, 2H), 4.38 (s, 2H). ¹³C NMR (75 MHz, CDCl₃): δ 142.1, 132.6, 126.4, 93.1, 6.8. *m/z* (EI): 256, 254, 252 (M⁺, 4, 16, 12%), 205, 203 (M-CH₂Cl, 100, 100%). HPLC: Column Symmetry C18, 5 μm , 100 \AA , (150 \times 3.9 mm), Purity 99%, r.t. = 4.73 min, acetonitrile/H₂O (0.05% H₃PO₄ + 0.04% Et₃N) 50/50.

General Procedure for Bromoacetyl Benzene (21, 23, 25, 27, and 29), Dibromoacetyl Benzene (22, 24, 26, 28), and Pyridine (30) Synthesis. To a solution of acetophenone derivative or 2-acetyl pyridine dissolved in CHCl₃ (35 mL) was added dropwise a solution of bromine in CHCl₃ (10 mL) at 0 °C. The mixture was stirred 2 h. The solvent was evaporated and to the mixture was added CH₂Cl₂ (50 mL) and a saturated solution of NaHCO₃ (50 mL). The organic layer was dried over MgSO₄ and the solvent was evaporated. Compounds were purified/separated by silica gel chromatography.

4-(2-Bromoacetyl)benzonitrile (21).⁴³ and 4-(2,2-Dibromoacetyl)benzonitrile (22).⁴⁴ 4-Acetylbenzonitrile (1.0 g, 6.89 mmol), bromine (1.12 g, 7.02 mmol). Mixture of compounds separated by silica gel chromatography (hexane:ethyl acetate 3:1), 0.69 g (45%) (21), colorless solid, mp 90–91 °C. ¹H NMR (200 MHz, CDCl₃): δ 8.10 (d, *J* = 8.79 Hz, 2H), 7.82 (d, *J* = 8.79 Hz, 2H), 4.44 (s, 2H). ¹³C NMR (75 MHz, CDCl₃): δ 190.4, 137.3, 133.0, 129.8, 118.0, 117.6, 30.4. *m/z* (EI): 225, 223 (M⁺, 4, 4%), 130 (M-COCH₂Br, 100%). HPLC: Column μ

Bondapack C18, 10 μm , 125 \AA , (300 \times 3.9 mm), Purity 97%, r.t. = 4.41 min, acetonitrile/H₂O (0.05% H₃PO₄ + 0.04% Et₃N) 50/50. Compound (22). 0.31 g (15%), colorless solid, mp 95–96 °C. ¹H NMR (200 MHz, CDCl₃): δ 8.23 (d, *J* = 8.79 Hz, 2H), 7.83 (d, *J* = 8.79 Hz, 2H), 6.58 (s, 1H). ¹³C NMR (75 MHz, CDCl₃): δ 185.0, 134.4, 132.9, 130.7, 117.9, 117.8, 39.0. *m/z* (EI): 305, 303, 301 (M⁺, 4, 12, 4%), 130 (M-COCHBr₂, 100%). HPLC: μ Bondapack C18, 10 μm , 125 \AA , (300 \times 3.9 mm), Purity 98%, r.t. = 4.11 min, acetonitrile/H₂O (0.05% H₃PO₄ + 0.04% Et₃N) 50/50.

2-Bromo-1-(4-(trifluoromethyl)phenyl)ethanone (23).⁴⁵ and 2,2-Dibromo-1-(4-(trifluoromethyl)phenyl)ethanone (24).⁴⁶ 1-(4-(Trifluoromethyl)phenyl) ethanone (1.0 g, 5.31 mmol), bromine (1.10 g, 6.90 mmol). Mixture of compounds separated by silica gel chromatography (hexane:ethyl acetate 8:1), 0.18 g (6%) (23), colorless solid, mp 55–56 °C. ¹H NMR (200 MHz, CDCl₃): δ 8.12 (d, *J* = 8.06 Hz, 2H), 7.79 (d, *J* = 8.06 Hz, 2H), 4.47 (s, 2H). ¹³C NMR (75 MHz, CDCl₃): δ 190.4, 136.5, 135.0 (q, *J*_{CF} = 33.09 Hz), 129.3, 125.9, 123.3. (q, *J*_{CF} = 272.9 Hz), 30.4. *m/z* (EI): 268, 266 (M⁺, 6, 6%), 172 (M-COCH₂Br, 100%). HPLC: Column μ Bondapack C18, 10 μm , 125 \AA , (300 \times 3.9 mm), Purity 97%, r.t. = 6.53 min, acetonitrile/H₂O (0.05% H₃PO₄ + 0.04% Et₃N) 50/50. Compound (24). 0.64 g (45%), colorless solid, mp 41–42 °C. ¹H NMR (200 MHz, CDCl₃): δ 8.22 (d, *J* = 8.3 Hz, 2H), 7.81 (d, *J* = 8.3 Hz, 2H), 6.6 (s, 1H). ¹³C NMR (75 MHz, CDCl₃): δ 184.1, 134.7 (q, *J* = 272.9 Hz), 132.7, 129.2, 124.8, 119.5 (q, *J* = 33.09), 38.2. *m/z* (EI): 348, 346, 344 (M⁺, 1, 6, 1%), 173 (M-CHBr₂, 100%). HPLC: Column μ Bondapack C18, 10 μm , 125 \AA , (300 \times 3.9 mm), Purity 97%, r.t. = 9.96 min, acetonitrile/H₂O (0.05% H₃PO₄ + 0.04% Et₃N) 50/50.

2-Bromo-1-(4-morpholinophenyl)ethanone (25).⁴⁷ 1-(4-Morpholinophenyl) ethanone (1.0 g, 4.87 mmol), bromine (1.01 g, 6.33 mmol). Purified by silica gel chromatography (hexane:ethyl acetate 1:1), 0.56 g (42%) (25), colorless solid, mp 108–109 °C. ¹H NMR (200 MHz, CDCl₃): δ 7.95 (d, *J* = 4 Hz, 2H), 7.04 (d, *J* = 4 Hz, 2H), 4.60 (s, 2H), 3.83 (m, 4H), 3.65 (m, 4H). ¹³C NMR (75 MHz, CDCl₃): δ 189.9, 154.9, 130.5, 120.3, 113.5, 67.8, 47.6, 26.7. *m/z* (EI): 285, 283 (M⁺, 14, 13%), 190 (M-CH₂Br, 100%). HPLC: Column μ Bondapack C18, 10 μm , 125 \AA , (300 \times 3.9 mm), Purity 99%, r.t. = 4.56 min, acetonitrile/H₂O (0.05% H₃PO₄ + 0.04% Et₃N) 50/50.

2,2-Dibromo-1-(4-iodophenyl)ethanone (26).⁴⁶ 1-(4-Iodophenyl)ethanone (0.40 g, 1.60 mmol), bromine (0.1 mL, 1.70 mmol). Purified by silica gel chromatography (hexane:ethyl acetate 6:1), 0.31 g (48%) (26), colorless solid, mp 77–78 °C. ¹H NMR (200 MHz, CDCl₃): δ 7.82 (d, *J* = 4.2 Hz, 2H), 7.73 (d, *J* = 4.2 Hz, 2H), 6.3 (s, 1H). ¹³C NMR (75 MHz, CDCl₃): δ 185.3, 138.6, 131.3, 130.4, 103.4, 39.6. *m/z* (EI): 406, 404, 402 (M⁺, 9, 17, 9%), 231, (M-CHBr₂, 100%). HPLC: Column Symmetry C18, 5 μm , 100 \AA , (150 \times 3.9 mm), Purity 98%, r.t. = 4.51 min, acetonitrile/H₂O (0.05% H₃PO₄ + 0.04% Et₃N) 50/50.

3-(2-Bromoacetyl)benzonitrile (27).⁴⁸ and 3-(2,2-Dibromoacetyl)benzonitrile (28).⁴⁹ 3-Acetylbenzonitrile (0.5 g, 3.44 mmol), bromine (0.72 g, 4.48 mmol). Mixture of compounds separated by silica gel chromatography (hexane:ethyl acetate 5:2), 0.10 g (13%) (27), colorless solid, mp 70–71 °C. ¹H NMR (200 MHz, CDCl₃): δ 8.21 (t, *J* = 1.5 Hz, 1H), 8.15 (td, *J* = 7.9, 1.5 Hz, 1H), 7.95 (td, *J* = 7.9, 1.5 Hz, 1H), 7.80 (t, *J* = 7.9 Hz, 1H), 4.32 (s, 2H). ¹³C NMR (75 MHz, CDCl₃): δ 189.8, 137.0, 135.1, 133.2, 133.0, 130.2, 117.9, 113.9, 30.1. *m/z* (EI): 225, 223 (M⁺, 2, 2%), 130 (M-CH₂Br, 100%). HPLC: Column μ Bondapack C18, 10 μm , 125 \AA , (300 \times 3.9 mm), Purity 97%, r.t. = 3.60 min, acetonitrile/H₂O (0.05% H₃PO₄ + 0.04% Et₃N) 50/50. Compound (28). 0.38 g (37%), colorless solid, mp 85–86 °C. ¹H NMR (200 MHz, CDCl₃): δ 8.25 (t, *J* = 1.5 Hz, 1H), 8.15 (td, *J* = 7.9, 1.5 Hz, 1H), 7.85 (td, *J* = 7.9, 1.5 Hz, 1H), 7.70 (t, *J* = 7.9 Hz, 1H), 6.40 (s, 1H, CH). ¹³C NMR (75 MHz, CDCl₃): δ 184.5, 137.4, 134.1, 133.8, 132.1, 130.2, 117.8, 114.0, 38.9. *m/z* (EI): 305, 303, 301 (M⁺, 3, 9, 3%), 130

(M-COCHBr₂, 100%). HPLC: Column μ Bondapak C18, 10 μ m, 125 Å, (300 \times 3.9 mm), Purity 98%, r.t. = 4.10 min, acetonitrile/H₂O (0.05% H₃PO₄ + 0.04% Et₃N) 50/50.

1-(4-Amino-3,5-dibromophenyl)-2-bromoethanone (**29**).⁴⁶ 1-(4-Aminophenyl) ethanone (0.5 g, 3.70 mmol), bromine (0.20 mL, 4.06 mmol). Purified by silica gel chromatography (hexane:ethyl acetate 2:1), 0.80 g (58%) (**29**), colorless solid, mp 146–147 °C. ¹H NMR (200 MHz, CDCl₃): δ 8.0 (s, 2H), 5.1 (s, 2H), 4.2 (s, 2H). ¹³C NMR (75 MHz, CDCl₃): δ 187.5, 147.3, 132.7, 123.3, 106.2, 38.3. *m/z* (EI): 375, 373, 371, 369 (M⁺, 10, 31, 31, 10%), 281, 279, 277 (M-CHBr₂, 64, 100, 67%). HPLC: Column Symmetry C18, 5 μ m, 100 Å, (150 \times 3.9 mm), Purity 96%, r.t. = 9.98 min, acetonitrile/H₂O (0.05% H₃PO₄ + 0.04% Et₃N) 50/50.

2,2-Dibromo-1-(pyridin-2-yl)ethanone (**30**).⁵⁰ 1-(Pyridin-2-yl)-ethanone (1.0 g, 8.25 mmol), bromine (1.45 g, 9.08 mmol). Purified by silica gel chromatography (hexane:ethyl acetate 6:1), 1.69 g (74%) (**30**), colorless solid, mp 196–197 °C. ¹H NMR (200 MHz, CDCl₃): δ 8.71 (m, 1H), 8.10 (m, 2H), 7.82 (m, 1H), 6.13 (s, 1H). ¹³C NMR (75 MHz, CDCl₃): δ 187.0, 149.5, 148.1, 138.4, 129.0, 124.0, 45.0. *m/z* (EI): 281, 279, 277 (M⁺, 9, 19, 9%), 106 (M-CHBr₂, 100%). HPLC: Column Symmetry C18, 5 μ m, 100 Å, (150 \times 3.9 mm), Purity 98%, r.t. = 3.66 min, acetonitrile/H₂O (0.05% H₃PO₄ + 0.04% Et₃N) 50/50.

1-(6-Amino-9H-purin-9-yl)ethanone (**31**).²³ To a solution of adenine (1.23 g, 9.14 mmol) in DMSO anhydrous (50 mL) was added a solution of pyridine anhydrous (20 mL) and acetic anhydride (5 mL). The mixture was stirred for 24 h at room temperature and a white precipitate formed. The precipitate was filtered and washed with several portions of cold pyridine and ether, to afford a white solid (629 mg, 51%), mp 363–364 °C. ¹H NMR (300 MHz, DMSO-*d*₆): δ 8.61 (s, 1H), 8.28 (s, 1H), 7.52 (s, 2H), 2.88 (s, 3H). ¹³C NMR (75 MHz, DMSO-*d*₆): δ 173.97, 162.01, 159.50, 154.36, 144.05, 125.17, 30.41. HPLC: Purity >99%, r.t. = 0.55 min. MS (ESI⁺): *m/z* 178 [M+H]⁺.

1-(6-Amino-9H-purin-9-yl)-2-chloroethanone (**32**). To a solution of adenine (1.00 g, 7.4 mmol) in THF anhydrous (50 mL) was added a mixture of pyridine anhydrous (20 mL) and chloroacetic anhydride (1.39 g, 8.14 mmol). The mixture was stirred for 24 h at room temperature and a white precipitate was formed. The precipitate was filtered and washed with several portions of cold pyridine and cold ether. This solid was purified by column chromatography (methanol:dichloromethane 1:10) to afford a white solid (312 mg, 20%), mp 199–200 °C. ¹H NMR (400 MHz, DMSO-*d*₆): δ 12.28 (s, 1H), 11.48 (s, 2H), 8.65 (s, 1H), 8.45 (s, 1H), 4.55 (s, 2H). ¹³C NMR (101 MHz, DMSO-*d*₆): δ 166.32, 151.25, 145.74, 144.20, 118.15, 43.40. HPLC: Purity 95%, r.t. = 2.87 min. MS (ESI⁺): *m/z* 212 [M+H]⁺.

1-(4-(4-Methoxyphenylamino)-3-nitrophenyl)ethanone (**33**).⁵¹ To a solution of 1-(4-bromo-3-nitrophenyl)ethanone (1 g, 4.09 mmol) and 4-methoxyaniline (0.504 g, 4.09 mmol) in anhydrous DMF (23 mL) was added sodium acetate (0.504 g, 6.14 mmol). The mixture was heated 2 h at 100 °C and then stirred at room temperature overnight. Ethyl acetate (100 mL) and H₂O (100 mL) was added to the reaction mixture. The organic layer was washed with H₂O (2 \times 100 mL), dried over MgSO₄, and the solvent was evaporated. The residue was recrystallized from MeOH/H₂O to afford **33** as a red solid (853 mg, 73%), mp 132–133 °C. ¹H NMR (300 MHz, CDCl₃): δ 9.77 (s, 1H), 8.82 (s, 1H), 7.94 (d, *J* = 8.9 Hz, 1H), 7.21 (d, *J* = 8.7 Hz, 2H), 7.10–6.83 (m, 3H), 3.86 (s, 3H), 2.58 (s, 3H). ¹³C NMR (75 MHz, CDCl₃): δ 194.7, 158.4, 147.6, 134.4, 131.1, 129.8, 128.4, 127.2, 126.1, 115.6, 115.1, 55.4, 25.92. HPLC: Purity >99%, r.t. = 5.09 min. MS (ESI⁺): *m/z* 287 [M+H]⁺.

1-(4-(4-Methoxyphenylamino)-3-aminophenyl)ethanone (**34**). To a solution of **33** (0.23 g, 0.8 mmol) dissolved in THF (20 mL) was added Pd(C) (23 mg). The mixture was stirred at room temperature overnight at 20 psi. The mixture was filtered and the solvent was evaporated to afford a brown solid. The title compound was used in the next step

without further purification. ¹H NMR (300 MHz, CDCl₃): δ 7.43 (m, 1H), 7.40 (s, 1H), 7.37 (m, 1H), 7.26 (m, 1H), 6.96–6.86 (m, 2H), 6.86–6.68 (m, 2H), 5.64 (s, 1H), 3.81 (s, 3H), 2.51 (s, 3H), 1.44 (s, 1H). HPLC: Purity 88%, r.t. = 4.15 min. MS (ESI⁺): *m/z* 257 [M+H]⁺.

1-(1-(4-Methoxyphenyl)-1H-benzo[d]imidazol-5-yl)ethanone (**35**). A stirred solution of **34** (0.93 g, 3.64 mmol) and formic acid (1.58 mL, 42 mmol) in HCl 4 N (25 mL) was refluxed for 3 h. Then dichloromethane (25 mL) was added to the mixture. The organic layer was washed with saturated NaHCO₃ solution (3 \times 25 mL) and then dried over MgSO₄. The solvent was evaporated under reduced pressure to give **35** as a brown solid (803 mg, 83%), mp 139–140 °C. ¹H NMR (300 MHz, CDCl₃): δ 8.46 (d, *J* = 1.1 Hz, 1H), 8.13 (s, 1H), 7.99 (dd, *J* = 8.6, 1.5 Hz, 1H), 7.50–7.42 (m, 1H), 7.40 (d, *J* = 9.0 Hz, 2H), 7.08 (d, *J* = 9.0 Hz, 2H), 3.89 (s, 3H), 2.69 (s, 3H). ¹³C NMR (75 MHz, CDCl₃): δ 198.0, 159.9, 144.6, 132.6, 128.7, 126.0, 123.9, 122.4, 115.5, 110.6, 55.9, 26.9. HPLC: Purity 99%, r.t. = 4.18 min. MS (ESI⁺): *m/z* 267 [M+H]⁺.

2-Bromo-1-(1-(4-methoxyphenyl)-1H-benzo[d]imidazol-5-yl)ethanone (**36**). To a solution of **35** (1.14 g, 4.28 mmol) dissolved in AcOH (25 mL) at reflux was added a solution of bromine (0.23 mL, 4.50 mmol) in AcOH (5 mL). The mixture was refluxed and stirred for 5 h. Dichloromethane (50 mL) and water (50 mL) were added to the mixture. The organic layer was extracted and washed with saturated solutions of NaHCO₃ (2 \times 50 mL) and NaCl (50 mL). The organic layer was dried over MgSO₄ and the solvent was evaporated. The product was purified by flash chromatography (hexane:ethyl acetate 1:1), 162 mg (11%) (**36**), red solid, mp 247–248 °C. ¹H NMR (300 MHz, CDCl₃): δ 8.52 (s, *J* = 1.1 Hz, 1H), 8.18 (s, 1H), 8.03 (dd, *J* = 8.6, 1.6 Hz, 1H), 7.51 (d, *J* = 8.6, 1H), 7.41 (d, *J* = 9.0 Hz, 2H), 7.10 (d, *J* = 9.0 Hz, 2H), 4.57 (s, 2H), 3.91 (s, 3H). ¹³C NMR (75 MHz, CDCl₃): δ 191.2, 160.0, 144.9, 126.0, 124.7, 122.9, 115.5, 111.1, 55.9. HPLC: Purity 95%, r.t. = 4.70 min. MS (ESI⁺): *m/z* 345 [M+H]⁺.

General Procedure for Maleimide Synthesis (**37–38**). To a solution of acetoacetamide (1 equiv) and ^tBuOK (1 M solution in THF) (3.5 equiv) dissolved in THF (20 mL) at –60 °C was added methyl 3-indoleglyoxylate or methyl 2-(1-methyl-1H-indol-3-yl)-2-oxoacetate (1 equiv). The mixture was stirred until room temperature was reached. Then a concentrated HCl solution (11.5 mL), water (30 mL), and dichloromethane (30 mL) were added in the reaction mixture. The organic layer was washed with a saturated solution of NaHCO₃ (2 \times 30 mL), dried over MgSO₄, and evaporated. Products were purified by recrystallization from ethyl acetate/pentane.

3-Acetyl-4-(1H-indol-3-yl)-1H-pyrrole-2,5-dione (**37**). Acetoacetamide (0.372 g, 3.69 mmol), ^tBuOK (1 M solution in THF) (12.9 mL, 12.9 mmol), methyl 3-indoleglyoxylate (0.750 g, 3.69 mmol). 0.70 g (74%) (**37**), orange solid, mp 225–226 °C. ¹H NMR (300 MHz, DMSO-*d*₆): δ 12.29 (s, 1H), 11.17 (s, 1H), 8.24 (s, 1H), 7.50 (d, *J* = 7.01 Hz, 1H), 7.27–7.17 (m, 1H), 7.13 (s, 2H), 2.50–2.46 (s, 3H). ¹³C NMR (75 MHz, DMSO-*d*₆): δ 195.4, 171.7, 139.8, 137.5, 135.5, 125.5, 124.9, 123.5, 122.6, 121.7, 113.3, 106.0, 31.7. HPLC/MS: Purity >99%, r.t. = 3.76 min. MS (ESI⁺): *m/z* 255 [M+H]⁺.

3-Acetyl-4-(1-methyl-indol-3-yl)-1H-pyrrole-2,5-dione (**38**). Acetoacetamide (0.325 g, 3.22 mmol), ^tBuOK (1 M solution in THF) (11.3 mL, 11.3 mmol), 2-(1-methyl-1H-indol-3-yl)-2-oxoacetate (0.700 g, 3.22 mmol). 0.482 g (56%) (**38**), red solid, mp 224–225 °C. ¹H NMR (300 MHz, DMSO-*d*₆): δ 11.19 (s, 1H), 8.27 (s, 1H), 7.58 (d, *J* = 8.1 Hz, 1H), 7.35–7.06 (m, 3H), 3.92 (s, 3H), 2.51 (s, 3H). ¹³C NMR (75 MHz, DMSO-*d*₆): δ 194.6, 170.9, 138.5, 138.1, 137.3, 125.2, 123.8, 122.8, 122.1, 121.3, 111.0, 104.3, 33.3, 30.9. HPLC/MS: Purity 95%, r.t. = 4.06 min. MS (ESI⁺): *m/z* 269 [M+H]⁺.

General Procedure for Maleimide Bromination (**39 and 40**). Maleimide derivative **37** or **38** (1 equiv) is dissolved in AcOH. Under reflux conditions, bromine (1.05 equiv) is slowly added diluted in AcOH. The mixture is stirred at reflux temperature for 3 h. Then water and AcOEt are added and the mixture is extracted, and the organic layer washed with

several portions of a NaHCO₃ saturated solution and then dried and evaporated. The products are purified by recrystallization MeOH/H₂O (39) or by flash chromatography (40) using a dichloromethane/methanol 80:1 mixture as eluent.

3-(2-Bromoacetyl)-4-(1H-indol-3-yl)-1H-pyrrole-2,5-dione (39). Title compound was prepared using the same procedure described for the synthesis of compound 36. Maleimide 37 (0.670 g, 2.63 mmol), bromine (0.135 mL, 2.63 mmol). The residue was recrystallized from methanol/water to give 39 as a black solid (0.345 g, 39%), mp 260–261 °C. ¹H NMR (300 MHz, DMSO-*d*₆): δ 12.54 (s, 1H), 11.34 (s, 1H), 8.39 (m, 1H), 7.54 (d, *J* = 8.0 Hz, 1H), 7.32–6.98 (m, 3H), 4.75 (s, 2H). ¹³C NMR (126 MHz, acetone-*d*₆): δ 186.0, 169.6, 169.4, 142.1, 135.9, 135.7, 124.7, 122.8, 121.0, 112.1, 106.4, 35.0. HPLC/MS: Purity 95%, r.t = 4.35 min. MS (ESI+): *m/z* 333 [M+H]⁺.

3-(2-Bromoacetyl)-4-(1-methyl-1H-indol-3-yl)-1H-pyrrole-2,5-dione (40). Title compound was prepared using the same procedure described for the synthesis of compound 36. Maleimide 38 (0.603 g, 2.25 mmol), bromine (0.115 mL, 2.25 mmol). The product was purified by flash chromatography (dichloromethane:methanol 80:1), 120 mg (15%) (40), purple solid, mp 252–253 °C. ¹H NMR (300 MHz, CDCl₃): δ 8.46 (s, 1H), 7.38 (m, 4H), 5.31 (s, 1H), 4.64 (s, 2H), 3.94 (s, 3H). ¹³C NMR (126 MHz, acetone-*d*₆): δ 185.80, 169.78, 169.55, 141.80, 139.52, 137.66, 125.37, 122.94, 122.88, 121.34, 119.28, 110.46, 105.53, 35.02, 32.71. HPLC: Purity 99%, r.t = 4.47 min. MS (ESI+): *m/z* 347 [M+H]⁺.

Chemical Reactivity of HMKs. 100 μL of an acetonitrile solution of HMK 3 or 4 (50 mM) and 100 μL of an acetonitrile solution of 2-mercaptoethanol (50 mM) were added to a mixture of methanol/water (1/1, 0.8 mL) and stirred for 1 or 18 h. The reaction progress was followed by HPLC-MS. HMK 3 (MW = 189) showed a retention time of 4.90 min, while retention time for HMK 4 (MW = 233) was 5.05 min. On the other hand, the S-alkylated derivative (MW = 214) presented a retention time of 4.15 min. An additional experiment was carried out when the 2-mercaptoethanol concentration was increased 10 times. In this case, 100 μL of an acetonitrile solution of 2-mercaptoethanol (500 mM) was added. The same procedure described above was followed when triethylamine was used; 100 μL of an acetonitrile solution of triethylamine (50 mM) was added to a methanol/water (1/1, 0.7 mL) solution.

MALDI-TOF Analyses. Human recombinant GSK-3β was purchased from Millipore (Millipore Iberica S.A.U.). A stock solution of 10 μg of the enzyme in MilliQ water (100 μL) was prepared. Compound 38 (17.8 mM) and compound 40 (10 μM) were dissolved in MeOH, then 1 μL of each compound solution was added to 10 μL of the enzyme stock solution reproducing IC₅₀ experimental conditions prior to MALDI-TOF analysis.

Biological Studies. Inhibition of GSK-3 (Radiometric Assay). GSK-3β enzyme (Sigma) was incubated with 15 μM of ATP, 0.2 μCi of [^γ-³²P]ATP, GS-1 substrate, and different concentrations of test compound. GSK-3β activity was assayed in 50 mM Tris, pH 7.5, 10 mM MgCl₂, 1 mM EGTA, and 1 mM EDTA buffer at 37 °C, in the presence of 15 mM GS-1 (substrate), 15 μM of ATP, 0.2 μCi of [^γ-³²P] ATP in a final volume of 12 μL. After 20 min of incubation at 37 °C, 4 μL aliquots of the supernatant were spotted onto 2 × 2 pieces of Whatman P81 phosphocellulose paper, and the filter was washed four times (at least 10 min each time) in 1% phosphoric acid. The dried filters were transferred into scintillation vials, and the radioactivity was measured in a liquid scintillation counter. Blank values were subtracted, and the GSK-3β activity was expressed in percentage of maximal activity. The IC₅₀ is defined as the concentration of each compound that reduces enzyme activity by 50% with respect to that without inhibitor present.

Inhibition of GSK-3 (Luminescent Assay). Human recombinant GSK-3β was purchased from Millipore (Millipore Iberica S.A.U.). The prephosphorylated polypeptide substrate was purchased from Millipore

(Millipore Iberica S.A.U.). Kinase-Glo Luminescent Kinase Assay was obtained from Promega (Promega Biotech Ibérica, SL). ATP and all other reagents were from Sigma-Aldrich (St. Louis, MO). Assay buffer contained 50 mM HEPES (pH 7.5), 1 mM EDTA, 1 mM EGTA, and 15 mM magnesium acetate.

The method of Baki et al.⁵² was followed for the inhibition of GSK-3β. Kinase-Glo assays were performed in assay buffer using black 96-well plates. In a typical assay, 10 μL (10 μM) of test compound (dissolved in dimethyl sulfoxide [DMSO] at 1 mM concentration and diluted in advance in assay buffer to the desired concentration) and 10 μL (20 ng) of enzyme were added to each well followed by 20 μL of assay buffer containing 25 μM substrate and 1 μM ATP. The final DMSO concentration in the reaction mixture did not exceed 1%. After a 30 min incubation at 30 °C, the enzymatic reaction was stopped with 40 μL of Kinase-Glo reagent. Glow-type luminescence was recorded after 10 min using a FLUOstar Optima (BMG Labtechnologies GmbH, Offenburg, Germany) multimode reader. The activity is proportional to the difference of the total and consumed ATP. The inhibitory activities were calculated on the basis of maximal activities measured in the absence of inhibitor. The IC₅₀ was defined as the concentration of each compound that reduces a 50% the enzymatic activity with respect to that without inhibitors.

GSK-3 Reversibility Studies. To study the type of enzymatic inhibition for the compounds, assays were performed to determine the activity of the enzyme after several times of incubation of the enzyme with the inhibitor. A reversible inhibitor does not increase the inhibition of the enzyme with the time of incubation, while an irreversible inhibitor increases the inhibition percentage as it increases the time of incubation with the enzyme.

Antibodies and Western Blot Analysis. The antibodies used in this study were: anti-β-actin mAb (Sigma); PHF-1, which is an antiphospho Ser^{396/404} Tau mAb and Tau monoclonal antibody Tau-1, from Chemicon, that recognizes residues Ser 195, 198, 199, 202 non-phosphorylated.

Cell extracts were prepared from cells washed with 1 × PBS and then resuspended in a buffer containing the following: 20 mM HEPES, pH 7.4; 100 mM NaCl; 100 mM NaF; 1 mM sodium *ortho*-vanadate; 5 mM EDTA; Okadaic Acid 1 μM; 1% Triton X-100; and a protease inhibitor cocktail (Complete, Roche). The soluble fraction was obtained by centrifugation at 14000 g for 10 min at 4 °C, and the proteins (10–50 μg) were separated by SDS-PAGE before being transferred to a nitrocellulose filter. The filters were blocked with 5% nonfat milk in PBS and 0.1% Tween-20 (PBS-T) and then incubated with primary antibodies overnight at 4 °C. Subsequently, the filters were rinsed three times in PBST buffer before being exposed to the corresponding peroxidase-conjugated secondary antibody (diluted 1:5000, Promega) for 1 h at room temperature. Immunoreactivity was visualized using an enhanced chemiluminescence detection system (Perkin-Elmer Life Sci.). Each experiment was normalized with respect to the amount of actin present in each cell extract. The data are expressed as the mean of three independent experiments and the data from control cells were considered 100 relative unit (r.u.).

Inhibition of Protein Kinases. The experimental procedures for the inhibition of different protein kinases are described in each paragraph:

- Abl kinase:⁵³ Mouse recombinant (*E.coli*), staurosporine was used as reference compound and poly GT (0.4 μg.mL⁻¹) as a substrate. Fluorescence polarization was used as the method of detection for the reaction product (phosphopoly GT).
- CAM kinase II:⁵⁴ From rat brain, staurosporine was used as reference compound and [^γ³³-P] ATP + autocalmid-2 (5 μM) as a substrate. Liquid scintillation was used as method of detection for the reaction product ([^γ³³-P] autocalmid-2).
- EGFR kinase:⁵⁵ From A-431 cells, PD 153035 was used as reference compound and [^γ³³-P] ATP + poly GAT (0.48 mg.mL⁻¹) as a substrate. Liquid scintillation was used as method of detection for the reaction product ([^γ³³-P] poly GAT).

- IRK (*h*):⁵⁶ Human recombinant, staurosporine was used as reference compound and [γ^{33} -P] ATP + poly GT (0.03 mg.mL⁻¹) as a substrate. Liquid scintillation was used as method of detection for the reaction product ([γ^{33} -P] poly GT).
- MAP kinase (ERK 42):⁵⁷ Rat recombinant (*E.coli*), staurosporine was used as reference compound and [γ^{33} -P] ATP + MBP (0.5 mg.mL⁻¹) as a substrate. Liquid scintillation was used as method of detection for the reaction product ([γ^{33} -P] MBP).
- MEK1 kinase:⁵⁸ Rabbit recombinant (*E.coli*), staurosporine was used as reference compound and ATP + unactivated MAP kinase (0.01 mg.mL⁻¹) as a substrate. Liquid scintillation was used as method of detection for the reaction product ([γ^{33} -P] MBP).
- Protein kinase p56^{lck}:⁵⁹ From bovine thymus, staurosporine was used as reference compound and [γ^{33} -P] ATP + poliGT (0.5 mg.mL⁻¹) as a substrate. Liquid scintillation was used as method of detection for the reaction product ([γ^{33} -P] poliGT).

Neurotransmitter Receptors Binding Assays. The neurotransmitter binding assays are described in each paragraph:

- α -2 (non selective) adrenergic receptor:⁶⁰ From rat cerebral cortex, yohimbine was used as reference compound and [3 H] RX 821002 as a ligand (0.5 nM).
- D2 (*h*) dopamine receptor:⁶¹ Human recombinant (CHO cells), (+)-bucclamol was used as reference compound and [3 H] spiperone as a ligand (0.3 nM).
- D3 (*h*) dopamine receptor:⁶² Human recombinant (CHO cells), (+)-bucclamol was used as reference compound and [3 H] spiperone as a ligand (0.3 nM).
- AMPA glutaminergic receptor:⁶³ From rat cerebral cortex, L-glutamate was used as reference compound and [3 H] AMPA as a ligand (8 nM).
- NMDA glutaminergic receptor:⁶⁴ From rat cerebral cortex, CGS 19755 was used as reference compound and [3 H] CGP 39653 as a ligand (5 nM).
- M (nonselective) muscarinic receptor:⁶⁵ From rat cerebral cortex, atropine was used as reference compound and [3 H] QNB as a ligand (0.05 nM).
- N (neuronal) (α -BGTX-insensitive) nicotinic receptor:⁶⁶ From rat cerebral cortex, nicotine was used as reference compound and [3 H] cytosine as a ligand (1.5 nM).
- N (neuronal) (α -BGTX-sensitive) nicotinic receptor:⁶⁷ From rat cerebral cortex, α -bungarotoxin was used as reference compound and [125 I] α -bungarotoxin as a ligand (1 nM).
- 5-HT (nonselective) serotonergic receptor:⁶⁸ From rat cerebral cortex, serotonin was used as reference compound and [3 H] serotonin as a ligand (2 nM).

Molecular Modeling. Docking was performed with the program *rDock*, which is an extension of the program *RiboDock*,⁶⁹ using an empirical scoring function calibrated on the basis of protein–ligand complexes.⁷⁰ The reliability of *rDock* was assessed by docking a set of known GSK-3 inhibitors taking advantage of the X-ray crystallographic structures of their complexes with the enzyme (PDB entries 1J1B, 3F88, 1ROE, 1Q5K, 1UV5, and 2O5K; see Table S1 in Supporting Information). The docking of the novel HMK-containing adenine, benzimidazole, and maleimide derivatives was made using the X-ray structure of the original compounds that were designed (1J1B, 3F88, and 1ROE). The docking volume was defined as the space within 10 Å of the ligands found in those GSK-3 complexes. The structure of the ligands was initially energy minimized at the AM1⁷¹ level using *Gaussian 03*.⁷² Each compound was subjected to 100 docking runs, and the output docking modes were analyzed by visual inspection in conjunction with the docking scores.

■ ASSOCIATED CONTENT

● **Supporting Information.** Poses for selected GSK-3 inhibitors upon docking to their targets; docked poses for

derivatives of adenine (32) and maleimide (40) containing the halomethylketone moiety; elemental analyses of compounds. This material is available free of charge via the Internet at <http://pubs.acs.org>.

■ AUTHOR INFORMATION

Corresponding Author

*Phone: +34 91 5680010. Fax: +34 91 5644853. E-mail: amartinez@iqm.csic.es.

■ ACKNOWLEDGMENT

Financial support from MICINN and ISCiii (projects nos. SAF2009-13015-CO2-01, SAF2008-05595, SAF2006-01249 and RD07-0060/0015) and computational facilities from the CESCA are also acknowledged. D. I. P. acknowledges a post-doctoral grant to the CSIC (JAEDoc program) and V. P. a predoctoral grant (JAEPRe program).

■ ABBREVIATIONS

GSK-3, glycogen synthase kinase 3; CNS, central nervous system; AD, Alzheimer's disease; HMK, halomethylketone; TDZD, thiadiazolidindione; CDK-*n*, cyclin dependent kinase *n*, where *n* is 1, 2 or 5; GS-1, glycogen synthase 1; PDB, protein data bank; PK, protein kinase

■ REFERENCES

- (1) Cohen, P. Protein kinases—the major drug targets of the twenty-first century? *Nat Rev. Drug Discovery* **2002**, *1*, 309–315.
- (2) Duckett, D. R.; Cameron, M. D. Metabolism considerations for kinase inhibitors in cancer treatment. *Expert Opin. Drug Metab. Toxicol.* **2010**, *6*, 1175–1193.
- (3) Belani, C. P. The role of irreversible EGFR inhibitors in the treatment of non-small cell lung cancer: overcoming resistance to reversible EGFR inhibitors. *Cancer Invest.* **2010**, *28*, 413–423.
- (4) Chico, L. K.; Van Eldik, L. J.; Watterson, D. M. Targeting protein kinases in central nervous system disorders. *Nat. Rev. Drug Discovery* **2009**, *8*, 892–909.
- (5) Martinez, A.; Castro, A. Inhibition of tau phosphorylation: A new therapeutical strategy for the treatment of Alzheimer's disease and other neurodegenerative disorders. *Expert Opin. Ther. Pat.* **2000**, *10*, 1519–1527.
- (6) Plattner, F.; Angelo, M.; Giese, K. P. The roles of cyclin-dependent kinase 5 and glycogen synthase kinase 3 in tau hyperphosphorylation. *J. Biol. Chem.* **2006**, *281*, 25457–25465.
- (7) Perez, D. I.; Gil, C.; Martinez, A. Tau protein kinases inhibitors: from the bench to the clinical trials. In *Emerging Drugs and Targets for Alzheimer's Disease*, Martinez, A., Ed.; Royal Society of Chemistry: Cambridge, 2010; Vol. 1, pp 173–194.
- (8) Martinez, A.; Perez, D. I. GSK-3 inhibitors: a ray of hope for the treatment of Alzheimer's disease? *J Alzheimers Dis.* **2008**, *15*, 181–191.
- (9) Martinez, A. Preclinical efficacy on GSK-3 inhibitors: towards a future generation of powerful drugs. *Med. Res. Rev.* **2008**, *28*, 773–796.
- (10) Hooper, C.; Killick, R.; Lovestone, S. The GSK3 hypothesis of Alzheimer's disease. *J. Neurochem.* **2008**, *104*, 1433–1439.
- (11) Sereno, L.; Coma, M.; Rodriguez, M.; Sanchez-Ferrer, P.; Sanchez, M. B.; Gich, I.; Agullo, J. M.; Perez, M.; Avila, J.; Guardia-Laguarta, C.; Clarimon, J.; Lleó, A.; Gomez-Isla, T. A novel GSK-3beta inhibitor reduces Alzheimer's pathology and rescues neuronal loss in vivo. *Neurobiol. Dis.* **2009**, *35*, 359–367.
- (12) Peng, J.; Kudrimoti, S.; Prasanna, S.; Odde, S.; Doerksen, R. J.; Pennaka, H. K.; Choo, Y. M.; Rao, K. V.; Tekwani, B. L.; Madgula, V.; Khan, S. I.; Wang, B.; Mayer, A. M.; Jacob, M. R.; Tu, L. C.; Gertsch, J.;

Hamann, M. T. Structure-activity relationship and mechanism of action studies of manzamine analogues for the control of neuroinflammation and cerebral infections. *J. Med. Chem.* **2010**, *53*, 61–76.

(13) Hamann, M.; Alonso, D.; Martin-Aparicio, E.; Fuertes, A.; Perez-Puerto, M. J.; Castro, A.; Morales, S.; Navarro, M. L.; Del Monte-Millan, M.; Medina, M.; Pennaka, H.; Balaiah, A.; Peng, J.; Cook, J.; Wahyuono, S.; Martinez, A. Glycogen synthase kinase-3 (GSK-3) inhibitory activity and structure-activity relationship (SAR) studies of the manzamine alkaloids. Potential for Alzheimer's disease. *J. Nat. Prod.* **2007**, *70*, 1397–1405.

(14) Eldar-Finkelman, H.; Licht-Murava, A.; Pietrovski, S.; Eisenstein, M. Substrate competitive GSK-3 inhibitors - strategy and implications. *Biochim. Biophys. Acta* **2010**, *1804*, 598–603.

(15) Castro, A.; Encinas, A.; Gil, C.; Brase, S.; Porcal, W.; Perez, C.; Moreno, F. J.; Martinez, A. Non-ATP competitive glycogen synthase kinase 3beta (GSK-3beta) inhibitors: study of structural requirements for thiadiazolidinone derivatives. *Bioorg. Med. Chem.* **2008**, *16*, 495–510.

(16) Martinez, A.; Alonso, M.; Castro, A.; Dorronsoro, I.; Gelpi, J. L.; Luque, F. J.; Perez, C.; Moreno, F. J. SAR and 3D-QSAR studies on thiadiazolidinone derivatives: exploration of structural requirements for glycogen synthase kinase 3 inhibitors. *J. Med. Chem.* **2005**, *48*, 7103–7112.

(17) Perez, D. I.; Conde, S.; Perez, C.; Gil, C.; Simon, D.; Wandosell, F.; Moreno, F. J.; Gelpi, J. L.; Luque, F. J.; Martinez, A. Thienylhalomethylketones: Irreversible glycogen synthase kinase 3 inhibitors as useful pharmacological tools. *Bioorg. Med. Chem.* **2009**, *17*, 6914–25.

(18) Mazanetz, M. P.; Fischer, P. M. Untangling tau hyperphosphorylation in drug design for neurodegenerative diseases. *Nat. Rev. Drug Discovery* **2007**, *6*, 464–479.

(19) Martinez, A.; Alonso, M.; Castro, A.; Perez, C.; Moreno, F. J. First non-ATP competitive glycogen synthase kinase 3 beta (GSK-3beta) inhibitors: thiadiazolidinones (TDZD) as potential drugs for the treatment of Alzheimer's disease. *J. Med. Chem.* **2002**, *45*, 1292–1299.

(20) Leproult, E.; Barluenga, S.; Moras, D.; Wurtz, J. M.; Winssinger, N. Cysteine mapping in conformationally distinct kinase nucleotide binding sites: application to the design of selective covalent inhibitors. *J. Med. Chem.* **2011**, *54*, 1347–1355.

(21) Conde, S.; Perez, D. I.; Martinez, A.; Perez, C.; Moreno, F. J. Thienyl and phenyl alpha-halomethyl ketones: new inhibitors of glycogen synthase kinase (GSK-3beta) from a library of compound searching. *J. Med. Chem.* **2003**, *46*, 4631–4633.

(22) Woodgett, J. R. Use of peptide substrates for affinity purification of protein-serine kinases. *Anal. Biochem.* **1989**, *180*, 237–241.

(23) Dutta, S. P.; Hong, C. I.; Tritsch, G. L.; Cox, C.; Parthasarthy, R.; Chheda, G. B. Synthesis and biological activities of some N6- and N9-carbamoyladenines and related ribonucleosides. *J. Med. Chem.* **1977**, *20*, 1598–1607.

(24) Palmer, B. D.; Smaill, J. B.; Boyd, M.; Boschelli, D. H.; Doherty, A. M.; Hamby, J. M.; Khatana, S. S.; Kramer, J. B.; Kraker, A. J.; Panek, R. L.; Lu, G. H.; Dahring, T. K.; Winters, R. T.; Showalter, H. D.; Denny, W. A. Structure-activity relationships for 1-phenylbenzimidazoles as selective ATP site inhibitors of the platelet-derived growth factor receptor. *J. Med. Chem.* **1998**, *41*, 5457–5465.

(25) Faul, M. M.; Winneroski, L. L.; Krumrich, C. A. A new one step synthesis of maleimides by condensation of glyoxylate esters with acetamides. *Tetrahedron Lett.* **1999**, *40*, 1109–1112.

(26) Polgar, T.; Baki, A.; Szendrei, G. I.; Keseru, G. M. Comparative virtual and experimental high-throughput screening for glycogen synthase kinase-3beta inhibitors. *J. Med. Chem.* **2005**, *48*, 7946–7959.

(27) Martínez, A.; Gil, C.; Palomo, V.; Pérez, C.; Perez, D. I. Inhibidores de GSK-3 útiles en enfermedades neurodegenerativas, inflamatorias, cáncer, diabetes y en procesos regenerativos. ES 201130253, 25th February, 2011.

(28) Kafka, A. P.; Kleffmann, T.; Rades, T.; McDowell, A. The application of MALDI TOF MS in biopharmaceutical research. *Int. J. Pharm.* **2011**, doi:10.1016/j.ijpharm.2010.12.010

(29) Kockeritz, L.; Doble, B.; Patel, S.; Woodgett, J. R. Glycogen synthase kinase-3—an overview of an over-achieving protein kinase. *Curr. Drug Targets* **2006**, *7*, 1377–1388.

(30) Li, T.; Paudel, H. K. Glycogen synthase kinase 3beta phosphorylates Alzheimer's disease-specific Ser396 of microtubule-associated protein tau by a sequential mechanism. *Biochemistry* **2006**, *45*, 3125–3133.

(31) Johnson, L. N. Protein kinase inhibitors: contributions from structure to clinical compounds. *Q. Rev. Biophys.* **2009**, *42*, 1–40.

(32) Hagel, M.; Niu, D.; St Martin, T.; Sheets, M. P.; Qiao, L.; Bernard, H.; Karp, R. M.; Zhu, Z.; Labenski, M. T.; Chaturvedi, P.; Nacht, M.; Westlin, W. F.; Petter, R. C.; Singh, J. Selective irreversible inhibition of a protease by targeting a noncatalytic cysteine. *Nat. Chem. Biol.* **2011**, *7*, 22–24.

(33) Shaw, W. G.; Brown, G. H. The mesomorphic state: The mesomorphic 4,4'-di(n)alkoxybenzalazines. *J. Am. Chem. Soc.* **1959**, *81*, 2532–2537.

(34) Hill, J. H. M. Mechanism of the Gabriel-Colman rearrangement. *J. Org. Chem.* **1965**, *30*, 620–622.

(35) Weng, Q.; Wang, D.; Guo, P.; Fang, L.; Hu, Y.; He, Q.; Yang, B. Q39, a novel synthetic Quinoxaline 1,4-Di-N-oxide compound with anti-cancer activity in hypoxia. *Eur. J. Pharmacol.* **2008**, *581*, 262–269.

(36) Roth, B.; Laube, R.; Tidwell, M. Y.; Rauckman, B. S. Extrusion of sulfur from [(acylmethyl)thio]pyrimidinones. *J. Org. Chem.* **1980**, *45*, 3651–3657.

(37) Zhuangping, Z.; Yongmin, Z.; Zhenghai, M. Indium-mediated reaction in aqueous media. Synthesis of phenacyl sulfides by reactions of a-bromoketones with sodium alkyl thiosulfates. *J. Chem. Res. Synopses* **1998**, *3*, 130–131.

(38) Kaila, N.; Janz, K.; DeBernardo, S.; Bedard, P. W.; Camphausen, R. T.; Tam, S.; Tsao, D. e. H. H.; Keith, J. C.; Nickerson-Nutter, C.; Shilling, A.; Young-Sciame, R.; Wang, Q. Synthesis and biological evaluation of quinoline salicylic acids as P-selectin antagonists. *J. Med. Chem.* **2006**, *50*, 21–39.

(39) Paizs, C.; To a, M.; Majdik, C.; Bóday, V.; Novák, L.; Irimie, F.-D.; Poppe, L. Chemo-enzymatic preparation of hydroxymethyl ketones. *J. Chem. Soc. Perkin Trans. 1* **2002**, *21*, 2400–2402.

(40) Nakaiida, S.; Kato, S.; Niyomura, O.; Ishida, M.; Ando, F.; Koketsu, J. Te-1-Acylmethyl and Te-1-Iminoalkyl Telluroesters: Synthesis and Thermolysis Leading to 1,3-Diketones and O-Alkenyl and O-Imino Esters. *Phosphorus, Sulfur Silicon Relat. Elem.* **2010**, *185*, 930–946.

(41) Artyomov, V. A.; Shestopalov, A. M.; Litvinov, V. P. Synthesis of Imidazo[1,2-a]pyridines from Pyridines and p-Bromophenacyl Bromide O-Methylxime. *Synthesis* **1996**, *8*, 927–929.

(42) Kim, Y. H.; Shin, H. H.; Park, Y. J. Facile one-pot synthesis of α -chloro sulfoxides from sulfides. *Synthesis* **1993**, 209–210.

(43) Kallmayer, H.-J.; Wagner, E. Zur Farbe der N-(4'-Nitrophenacyl)-arylamine. *Arch. Pharm.* **1980**, *313*, 315–323.

(44) Kyongtae, K.; Jaeeock, C.; Cheol, Y. S. Reactions of tetrasulfur tetranitride with aryl dibromomethyl ketones: one-pot synthesis of 3-aryloformamido-4-aryl-1,2,5-thiadiazoles and their reactions. *J. Chem. Soc. Perkin Trans. 1* **1995**, 253–260.

(45) Schröder, J.; Henke, A.; Wenzel, H.; Brandstetter, H.; Stammeler, H. G.; Stammeler, A.; Pfeiffer, W. D.; Tschesche, H. Structure-based design and synthesis of potent matrix metalloproteinase inhibitors derived from a 6H-1,3,4-thiadiazine scaffold. *J. Med. Chem.* **2001**, *44*, 3231–3243.

(46) Conde, S.; Martinez, A.; Perez, D. I.; Perez, C.; Moreno, F. J.; Wandosell, F. Compounds and their therapeutic use. US2003/199508 A1.

(47) Diwu, Z.; Beachdel, C.; Klaubert, D. H. A facile protocol for the convenient preparation of amino-substituted [alpha]-bromo- and [alpha],[alpha]-dibromo arylmethylketones. *Tetrahedron Lett.* **1998**, *39*, 4987–4990.

(48) Mathivanan, N.; Johnston, L. J.; Wayner, D. D. M. Photochemical generation of radical anions of photolabile aryl ketones. *J. Phys. Chem.* **1995**, *99*, 8190–8195.

(49) Watson, C. Y.; Wish, W. J. D.; Threadgill, M. D. Synthesis of 3-substituted benzamides and 5-substituted isoquinolin-1(2H)-ones and preliminary evaluation as inhibitors of poly(ADP-ribose)polymerase (PARP). *Bioorg. Med. Chem.* **1998**, *6*, 721–734.

- (50) Nobuta, T.; Hirashima, S.-i.; Tada, N.; Miura, T.; Itoh, A. Facile aerobic photo-oxidative syntheses of $[\alpha], [\alpha]$ -dibromoacetophenones from aromatic alkynes with 48% aq HBr. *Tetrahedron Lett.* **2010**, *51*, 4576–4578.
- (51) Kartinos, N.; Normington, J. B. Coloration of textile fibers with nitro keto arylamines. US 2708149 19550510.
- (52) Baki, A.; Bielik, A.; Molnar, L.; Szendrei, G.; Keseru, G. M. A high throughput luminescent assay for glycogen synthase kinase-3beta inhibitors. *Assay Drug Dev. Technol.* **2007**, *5*, 75–83.
- (53) Parker, G. J.; Law, T. L.; Lenocho, F. J.; Bolger, R. E. Development of high throughput screening assays using fluorescence polarization: nuclear receptor-ligand-binding and kinase/phosphatase assays. *J. Biomol. Screen.* **2000**, *5*, 77–88.
- (54) Lengyel, I.; Nairn, A.; McCluskey, A.; Toth, G.; Penke, B.; Rostas, J. Auto-inhibition of Ca(2+)/calmodulin-dependent protein kinase II by its ATP-binding domain. *J. Neurochem.* **2001**, *76*, 1066–1072.
- (55) Carpenter, G.; King, L., Jr.; Cohen, S. Rapid enhancement of protein phosphorylation in A-431 cell membrane preparations by epidermal growth factor. *J. Biol. Chem.* **1979**, *254*, 4884–4891.
- (56) Al-Hasani, H.; Passlack, W.; Klein, H. W. Phosphoryl exchange is involved in the mechanism of the insulin receptor kinase. *FEBS Lett.* **1994**, *349*, 17–22.
- (57) Robbins, D. J.; Zhen, E.; Owaki, H.; Vanderbilt, C. A.; Ebert, D.; Geppert, T. D.; Cobb, M. H. Regulation and properties of extracellular signal-regulated protein kinases 1 and 2 in vitro. *J. Biol. Chem.* **1993**, *268*, 5097–5106.
- (58) Williams, D. H.; Wilkinson, S. E.; Purton, T.; Lamont, A.; Flotow, H.; Murray, E. J. Ro 09–2210 exhibits potent anti-proliferative effects on activated T cells by selectively blocking MKK activity. *Biochemistry* **1998**, *37*, 9579–9585.
- (59) Cheng, H. C.; Nishio, H.; Hatase, O.; Ralph, S.; Wang, J. H. A synthetic peptide derived from p34cdc2 is a specific and efficient substrate of src-family tyrosine kinases. *J. Biol. Chem.* **1992**, *267*, 9248–9256.
- (60) Uhlen, S.; Wikberg, J. E. Rat spinal cord alpha 2-adrenoceptors are of the alpha 2A-subtype: comparison with alpha 2A- and alpha 2B-adrenoceptors in rat spleen, cerebral cortex and kidney using 3H-RX821002 ligand binding. *Pharmacol. Toxicol.* **1991**, *69*, 341–350.
- (61) Grandy, D. K.; Marchionni, M. A.; Makam, H.; Stofko, R. E.; Alfano, M.; Frothingham, L.; Fischer, J. B.; Burke-Howie, K. J.; Bunzow, J. R.; Server, A. C.; Cloning of the cDNA and gene for a human D2 dopamine receptor. *Proc. Natl. Acad. Sci. U.S.A.* **1989**, *86*, 9762–9766.
- (62) MacKenzie, R. G.; VanLeeuwen, D.; Pugsley, T. A.; Shih, Y. H.; Demattos, S.; Tang, L.; Todd, R. D.; O'Malley, K. L. Characterization of the human dopamine D3 receptor expressed in transfected cell lines. *Eur. J. Pharmacol.* **1994**, *266*, 79–85.
- (63) Murphy, D. E.; Snowhill, E. W.; Williams, M. Characterization of quisqualate recognition sites in rat brain tissue using DL-[3H]alpha-amino-3-hydroxy-5-methylisoxazole-4-propionic acid (AMPA) and a filtration assay. *Neurochem. Res.* **1987**, *12*, 775–781.
- (64) Sills, M. A.; Fagg, G.; Pozza, M.; Angst, C.; Brundish, D. E.; Hurt, S. D.; Wilusz, E. J.; Williams, M. [3H]CGP 39653: a new N-methyl-D-aspartate antagonist radioligand with low nanomolar affinity in rat brain. *Eur. J. Pharmacol.* **1991**, *192*, 19–24.
- (65) Richards, M. H. Rat hippocampal muscarinic autoreceptors are similar to the M2 (cardiac) subtype: comparison with hippocampal M1, atrial M2 and ileal M3 receptors. *Br. J. Pharmacol.* **1990**, *99*, 753–761.
- (66) Pabreza, L. A.; Dhawan, S.; Kellar, K. J. [3H]cytosine binding to nicotinic cholinergic receptors in brain. *Mol. Pharmacol.* **1991**, *39*, 9–12.
- (67) Sharples, C. G.; Kaiser, S.; Soliakov, L.; Marks, M. J.; Collins, A. C.; Washburn, M.; Wright, E.; Spencer, J. A.; Gallagher, T.; Whiteaker, P.; Wonnacott, S. UB-165: a novel nicotinic agonist with subtype selectivity implicates the alpha4beta2* subtype in the modulation of dopamine release from rat striatal synaptosomes. *J. Neurosci.* **2000**, *20*, 2783–2791.
- (68) Peroutka, S. J.; Snyder, S. H. Multiple serotonin receptors: differential binding of [3H]5-hydroxytryptamine, [3H]lysergic acid diethylamide and [3H]spiperidol. *Mol. Pharmacol.* **1979**, *16*, 687–699.
- (69) Morley, S. D.; Afshar, M. Validation of an empirical RNA-ligand scoring function for fast flexible docking using Ribodock. *J. Comput. Aided Mol. Des.* **2004**, *18*, 189–208.
- (70) Barril, X.; Hubbard, R. E.; Morley, S. D. Virtual screening in structure-based drug discovery. *Mini Rev. Med. Chem.* **2004**, *4*, 779–791.
- (71) Dewar, M. J. S.; Zoebisch, E. G.; Healy, E. F.; Stewart, J. J. P. Development and use of quantum mechanical molecular models. 76. AM1: a new general purpose quantum mechanical molecular model. *J. Am. Chem. Soc.* **1985**, *107*, 3902–3909.
- (72) Frisch, M. J.; Trucks, G. W.; Schlegel, H. B.; Scuseria, G. E.; Robb, M. A.; Cheeseman, J. R.; Montgomery, J. A., Jr.; Vreven, T.; Kudin, K. N.; Burant, J. C.; Millam, J. M.; Iyengar, S. S.; Tomasi, J.; Barone, V.; Mennucci, B.; Cossi, M.; Scalmani, G.; Rega, N.; Petersson, G. A.; Nakatsuji, H.; Hada, M.; Ehara, M.; Toyota, K.; Fukuda, R.; Hasegawa, J.; Ishida, M.; Nakajima, T.; Honda, Y.; Kitao, O.; Nakai, H.; Klene, M.; Li, X.; Knox, J. E.; Hratchian, H. P.; Cross, J. B.; Adamo, C.; Jaramillo, J.; Gomperts, R.; Stratmann, R. E.; Yazyev, O.; Austin, A. J.; Cammi, R.; Pomelli, C.; Ochterski, J. W.; Ayala, P. Y.; Morokuma, K.; Voth, G. A.; Salvador, P.; Dannenberg, J. J.; Zakrzewski, V. G.; Dapprich, S.; Daniels, A. D.; Strain, M. C.; Farkas, O.; Malick, D. K.; Rabuck, A. D.; Raghavachari, K.; Foresman, J. B.; Ortiz, J. V.; Cui, Q.; Baboul, A. G.; Clifford, S.; Cioslowski, J.; Stefanov, B. B.; Liu, G.; Liashenko, A.; Piskorz, P.; Komaromi, I.; Martin, R. L.; Fox, D. J.; Keith, T.; Al-Laham, M. A.; Peng, C. Y.; Nanayakkara, A.; Challacombe, M.; Gill, P. M. W.; Johnson, B.; Chen, W.; Wong, M. W.; Gonzalez, C.; Pople, J. A. *Gaussian 03*, rev B.04; Gaussian, Inc., Pittsburgh PA, 2003.